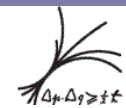




HERA Experience

Physics Aspects

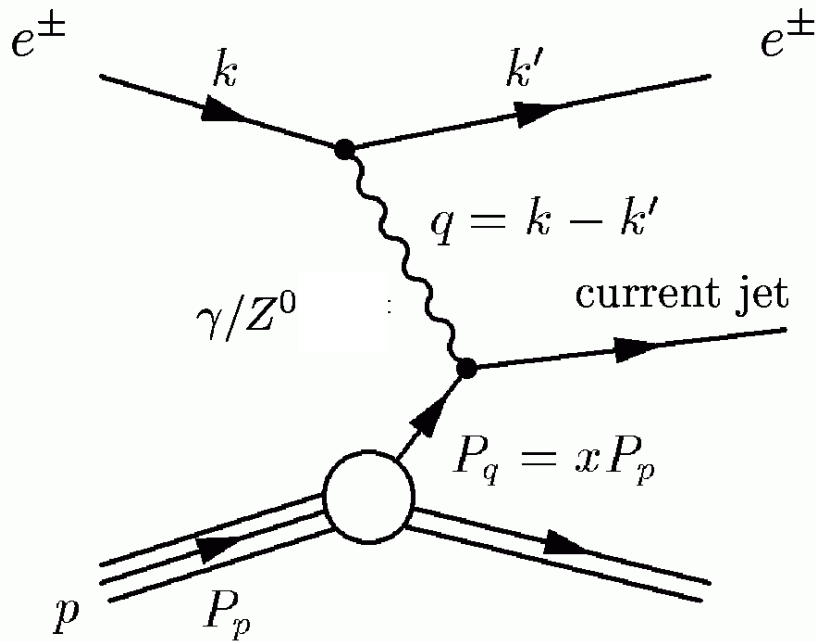
- DIS in collider mode:
Accelerator and Experiments
- HERA success story:
Precision cross sections, structure functions and parton densities
- HERA outlook:
What's still in the queue?
- Open Issues



MPI Munich

Burkard
Reisert
EINN 09
Milos

Deep Inelastic Scattering



Kinematic Variables

- 4-momentum transfer resolving power

$$Q^2 = -q^2 = -(k - k')^2$$

- Björken scaling variable momentum fraction of struck parton

$$x = \frac{Q^2}{2p \cdot q}$$

- Inelasticity:

$$y = \frac{p \cdot q}{p \cdot k}$$

Center of mass energy \sqrt{s} : $s = (k + p)^2$ relation for fixed s: $Q^2 = sxy$

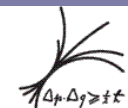
- Neutral current DIS cross section expressed by structure functions:

$$\frac{d^2 \sigma^{e^\pm p \rightarrow e^\pm X}}{dx dQ^2} = \frac{2\pi\alpha^2}{xQ^4} \underbrace{\left(1 + (1-y)^2\right)}_{Y_\pm = 1 \pm (1-y)^2} \cdot \left(F_2(x, Q^2) - \frac{y^2}{Y_+} F_L(x, Q^2) \mp \frac{Y_-}{Y_+} xF_3(x, Q^2) \right)$$

valence & sea quarks

gluons

valence quarks



MPI Munich

Burkard
Reisert

EINN 09

Milos

Mapping the Kinematic Plane

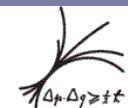
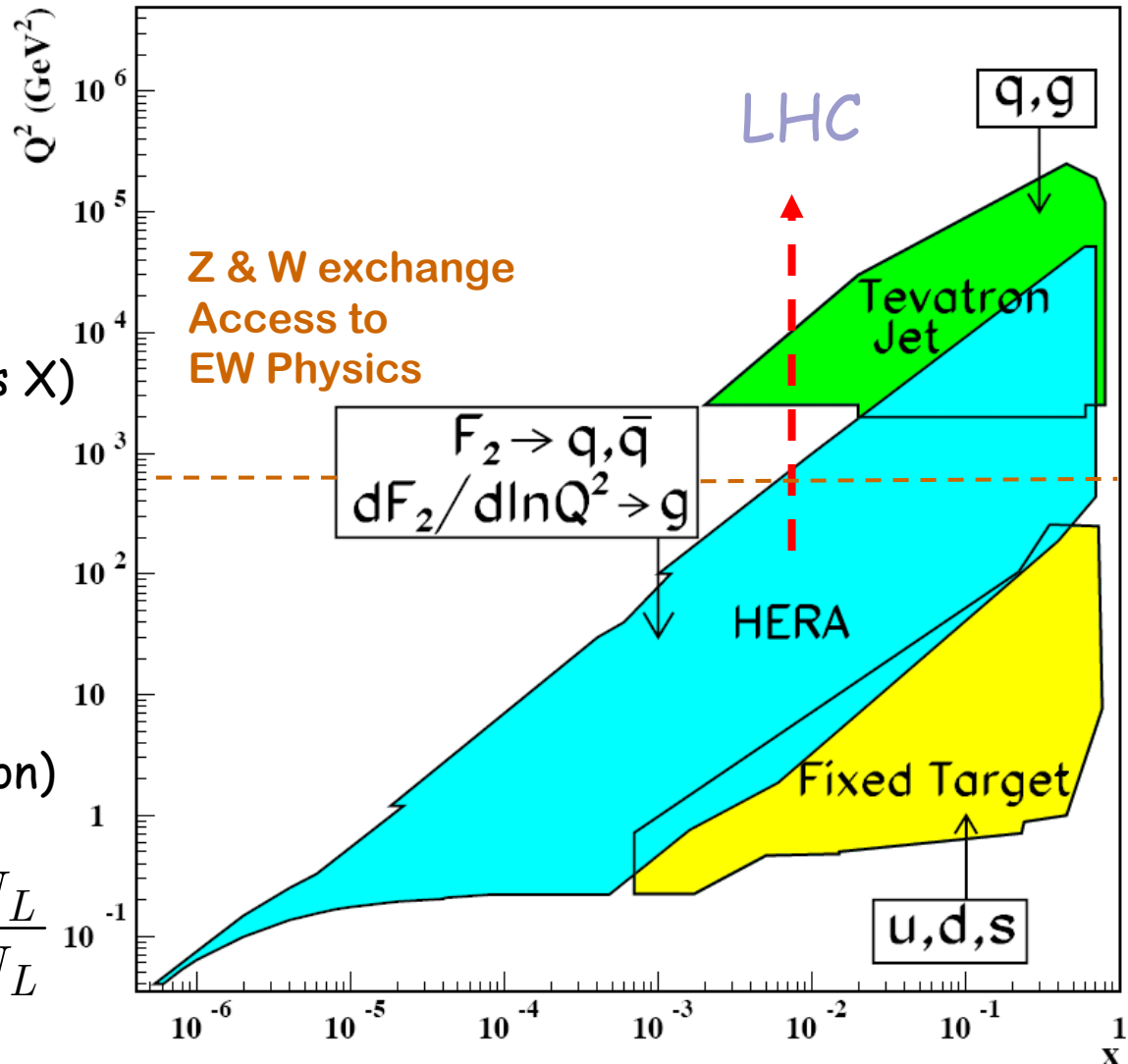
- large reach in x
- large reach in Q^2

“Inclusive” scattering
(integrate over all hadronic final states X)

- pdf's of quarks from F_2
- pdf of gluon from Q^2 variation of F_2 (e.g. DGLAP evolution)

$$\text{HERA II: } P_e = \frac{N_R - N_L}{N_R + N_L}$$

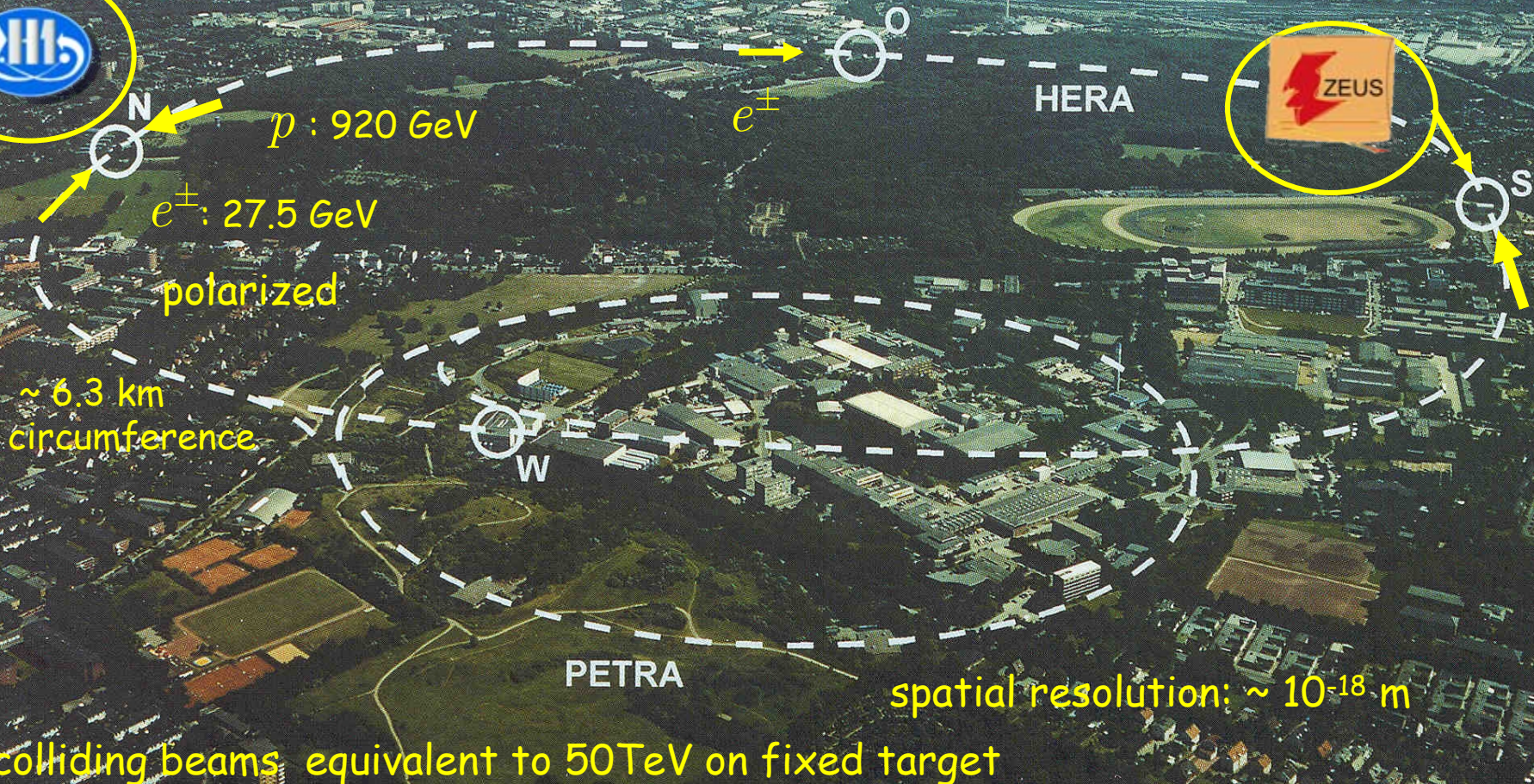
longitudinal polarization



HERA - the world's largest electron microscope (Deutsches Elektronen-Synchrotron DESY, Hamburg, Germany)

Shutdown on June 30, 2007, 23:00

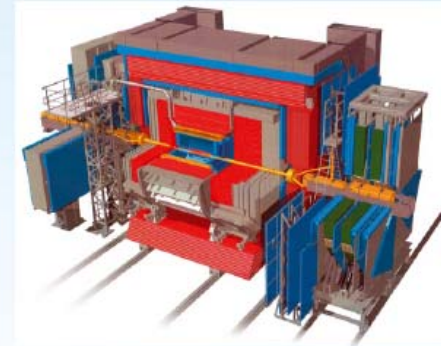
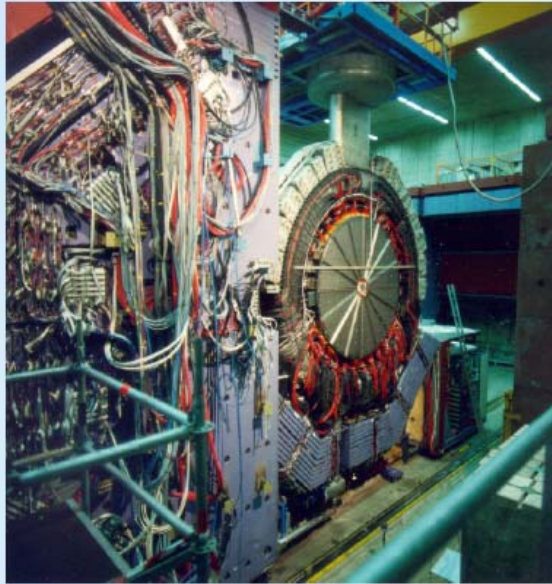
HERA start: 1992
upgraded in 2001: „HERA II“



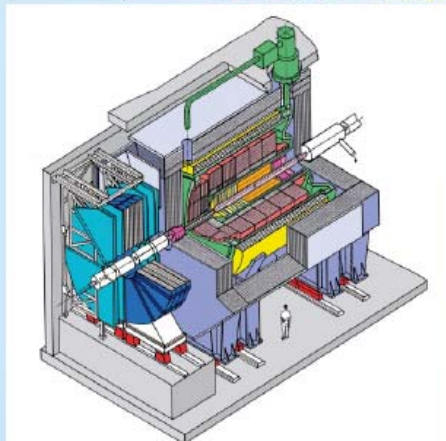
colliding beams equivalent to 50TeV on fixed target

Collider Experiments at HERA

H1
went
for
LAr

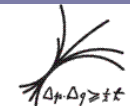
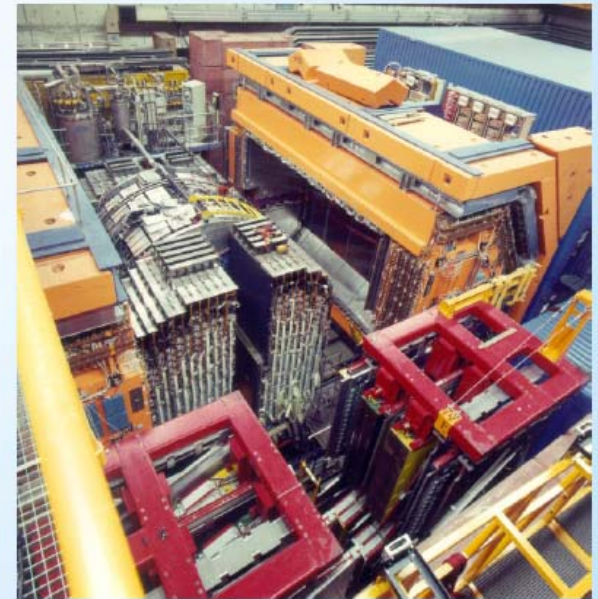


ZEUS
went
for
compensation



A final salute to
our experiments

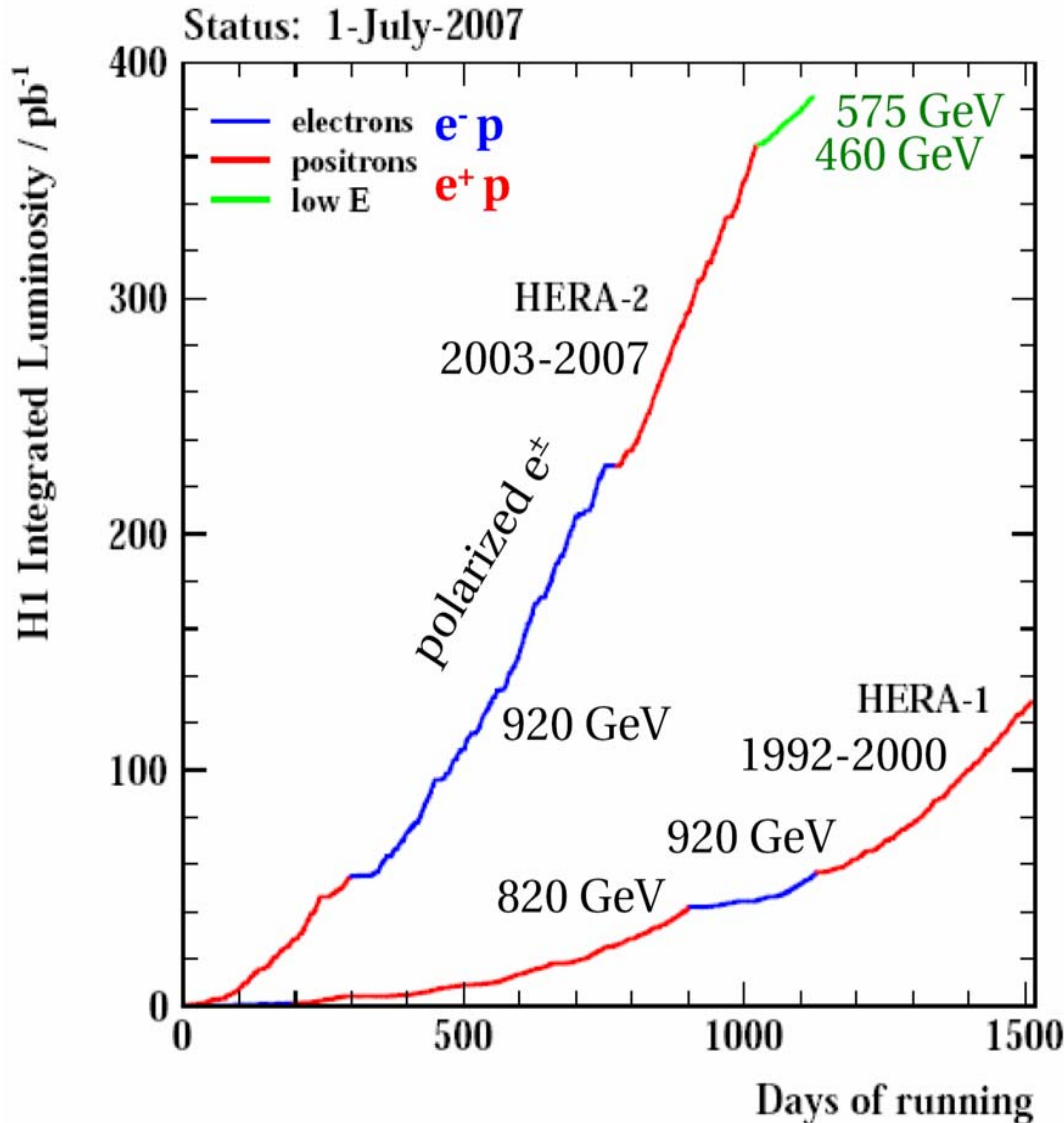
How we like to
remember
H1 and ZEUS



MPI Munich

Burkard
Reisert
EINN 09
Milos

Hera Luminosity



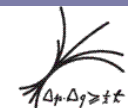
HERA I: 1992-2000

HERA II upgrade:

- luminosity
- longitudinal polarization of the lepton beams (spin rotator pairs around the interaction regions)
- massive upgrades also for the detectors



- running efficiently from 2003 onwards
- Luminosity
 $L = 500 \text{ pb}^{-1}$ per exp.

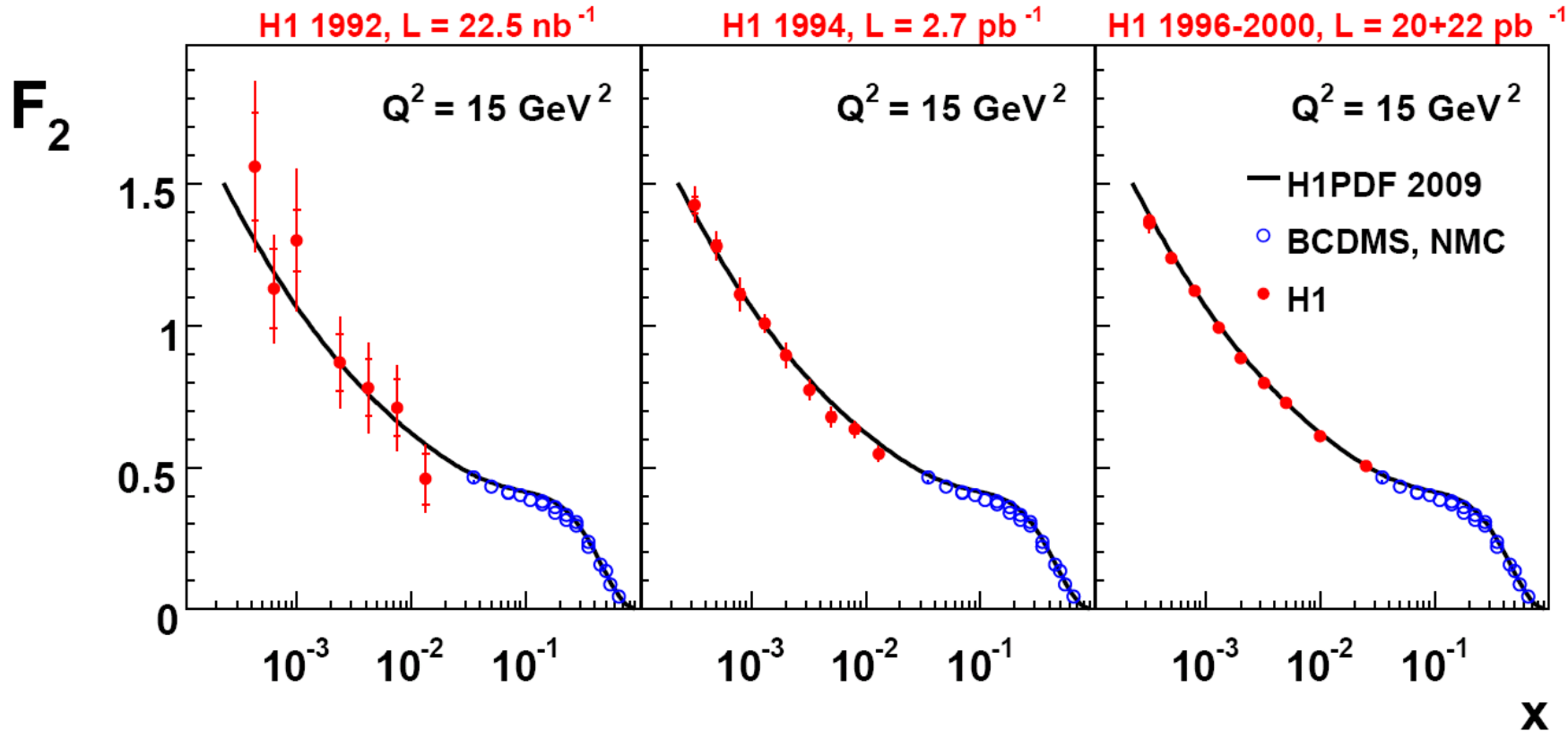


MPI Munich

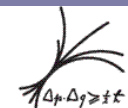
Burkard
Reisert
EINN 09
Milos

History of H1 F_2 Measurements

DIS 2009, Jan Kretzschmar, University of Liverpool – p.10



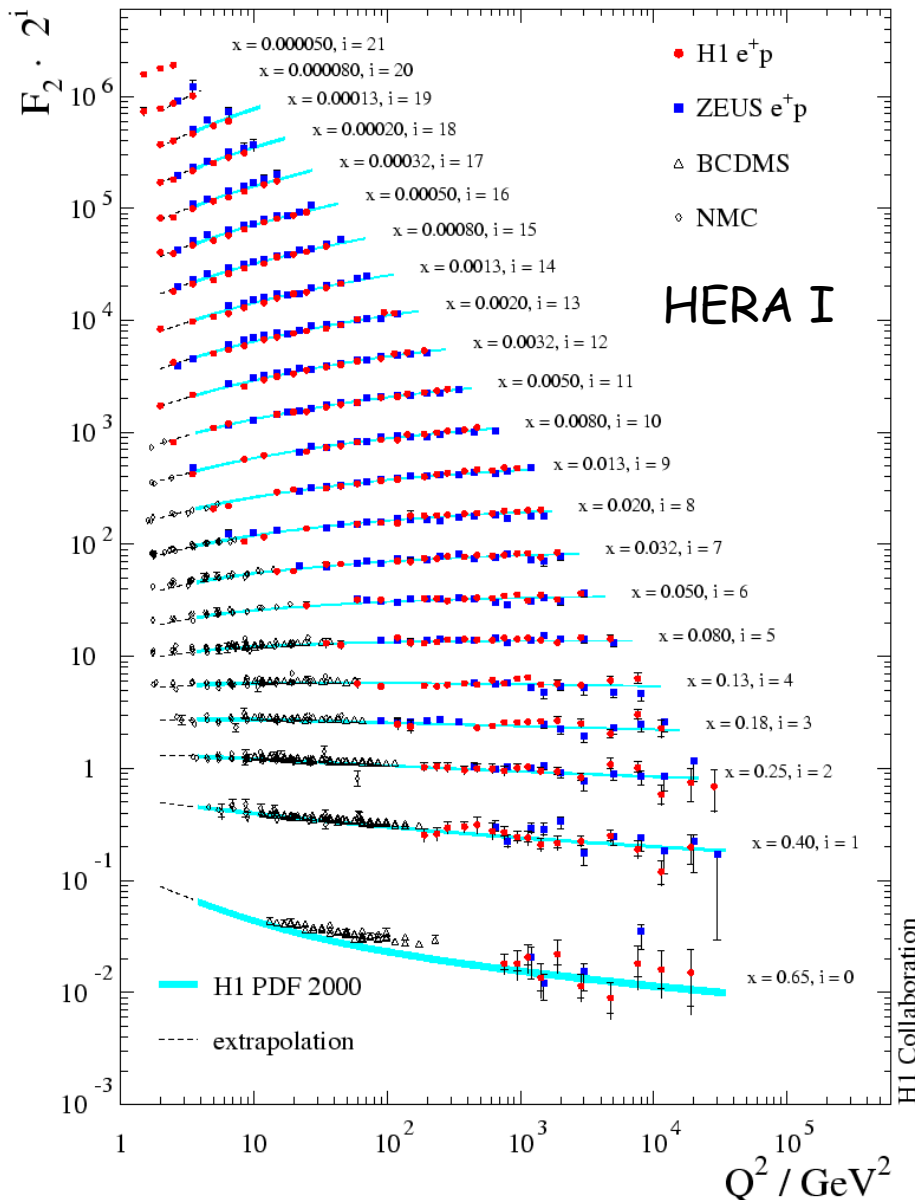
- Accuracies starting from 20 – 30%, reaching 4 – 6%, last publication using 1996/97 data 2 – 3%, and finally 1.3 – 2%



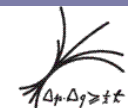
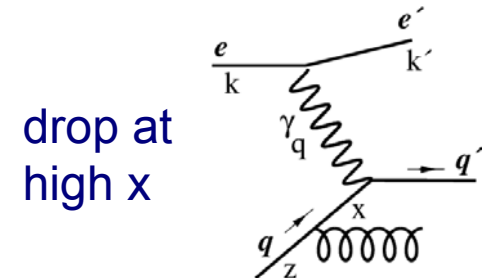
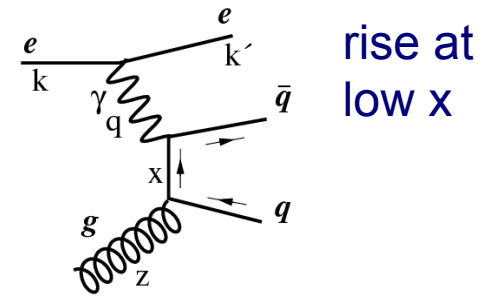
MPI Munich

Burkard
Reisert
EINN 09
Milos

Structure Function F_2



- H1 & ZEUS extended fixed target kinematic regime in x and Q^2 by 2 Orders
- Described by DGLAP
- Scaling violations



MPI Munich

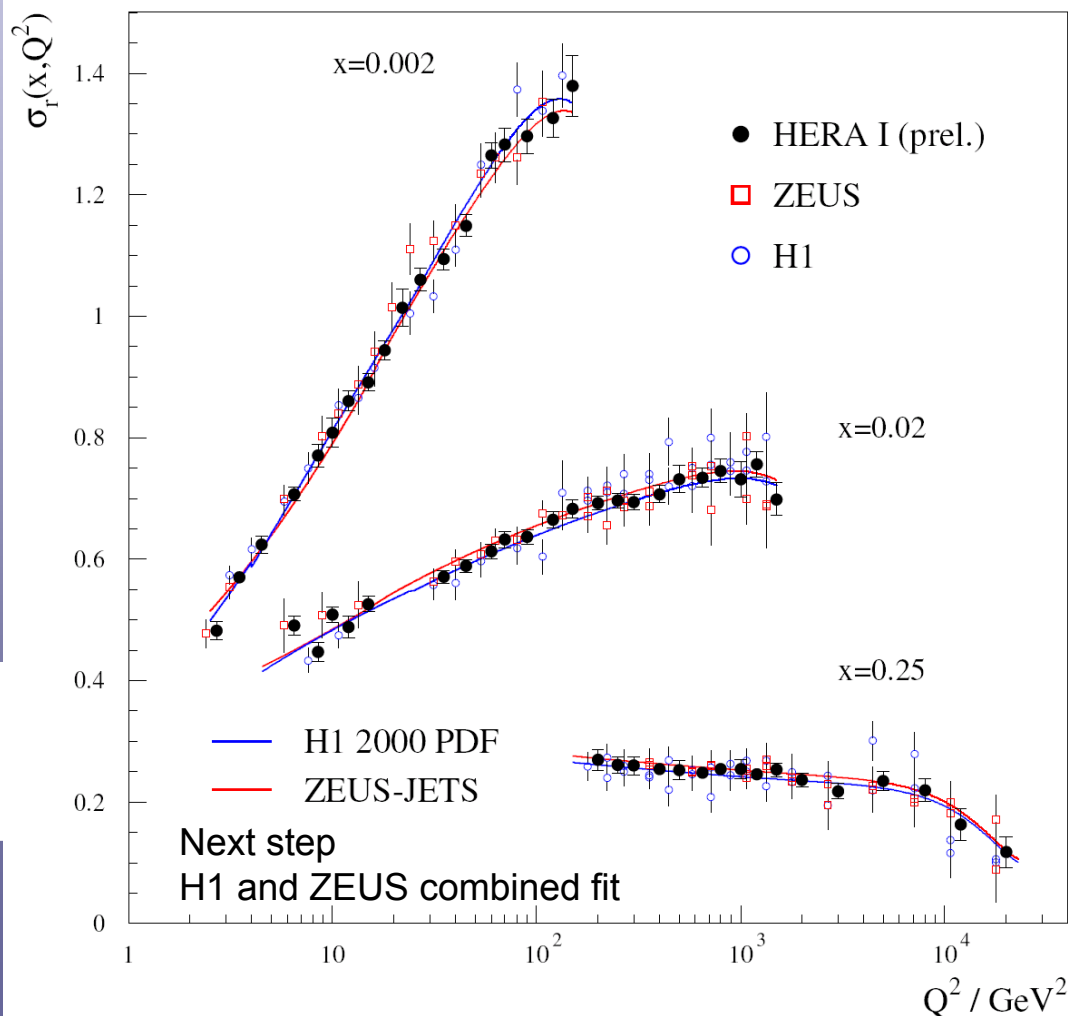
Burkard
Reisert

EINN 09
Milos

HERA Averaged NC cross sections

$$\sigma_r^{e^\pm p \rightarrow e^\pm X} = F_2 - \frac{y^2}{Y_+} F_L \mp \frac{Y_-}{Y_+} xF_3$$

HERA I e^+p Neutral Current Scattering - H1 and ZEUS



- Precise measurements from two experiments

- For $Q^2 \leq 100 \text{ GeV}^2$

$$\delta_{\text{stat}} \leq 1\%, \delta_{\text{sys}} \leq 3\%$$

- for $Q^2 \geq 1000 \text{ GeV}^2$

$$\delta_{\text{stat}} > \delta_{\text{sys}}$$

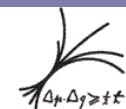
- Combine datasets from both experiments:

Key assumption

H1 and ZEUS measure the same cross section at the same x, Q^2, y

- Improved precision of combined H1 and ZEUS datasets (stat and sys)

HERA Structure Functions Working Group



MPI Munich

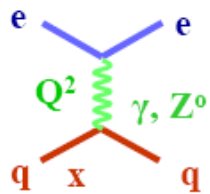
Burkard Reisert

EINN 09

Milos

Input to HERA PDF Fits

■ **NC**
$$\frac{d^2 \sigma^{e^\pm p \rightarrow e^\pm X}}{dx dQ^2} = \frac{2\pi\alpha^2}{xQ^4} \underbrace{\left(1 + (1-y)^2\right)}_{Y_\pm = 1 \pm (1-y)^2} \cdot \left(\tilde{F}_2(x, Q^2) - \frac{y^2}{Y_+} \tilde{F}_L(x, Q^2) \mp \frac{Y_-}{Y_+} x\tilde{F}_3(x, Q^2) \right)$$

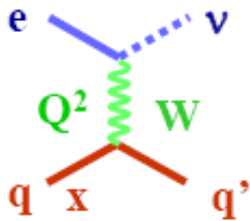


$$\tilde{F}_2 = \sum_i A_i(Q^2) [xq_i + x\bar{q}_i] \Rightarrow F_2^{em} = \frac{4}{9} x(u + \bar{u} + c + \bar{c}) + \frac{1}{9} x(d + \bar{d} + s + \bar{s})$$

$$x\tilde{F}_3 = \sum_i B_i(Q^2) [xq_i - x\bar{q}_i] \Rightarrow xF_3 = B_U x(u - \bar{u} + c - \bar{c}) + B_D x(d - \bar{d} + s - \bar{s})$$

Electroweak Coefficient Functions $A_i(Q^2)$, $B_i(Q^2)$ (QED: $A_i = e_i^2$)

■ **CC**

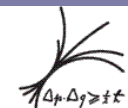


$$\sigma_{CC}(e^+ p) \propto x \left[(1-y^2)(d+s) + (\bar{u} + \bar{c}) \right] \times (1 + P_e)$$

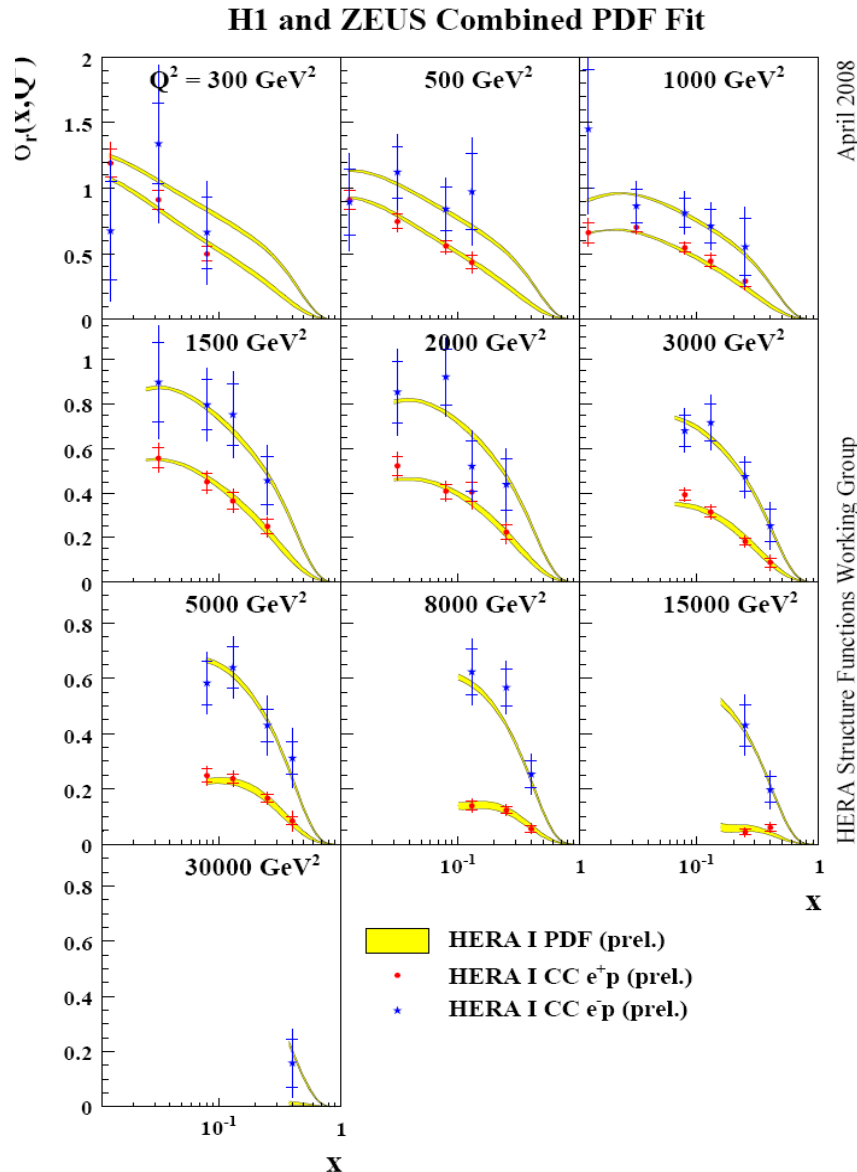
$$\sigma_{CC}(e^- p) \propto x \left[(u+c) + (1-y^2)(\bar{d} + \bar{s}) \right] \times (1 - P_e)$$

PDF general form: $xPDF = Ax^B (1-x)^C \cdot (1 + Dx + \dots)$

Parameterize: g , u_v , d_v , $\bar{U}(=\bar{u}+\bar{c})$, $\bar{D}(=\bar{d}+\bar{s})$



Charged Current Cross Section

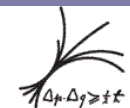


CC Cross section provide flavor sensible constrains at high x

$$\sigma_{CC}(e^+ p) \propto x \left[(1-y^2)D + \bar{U} \right]$$

$$\sigma_{CC}(e^- p) \propto x \left[U + (1-y^2)\bar{D} \right]$$

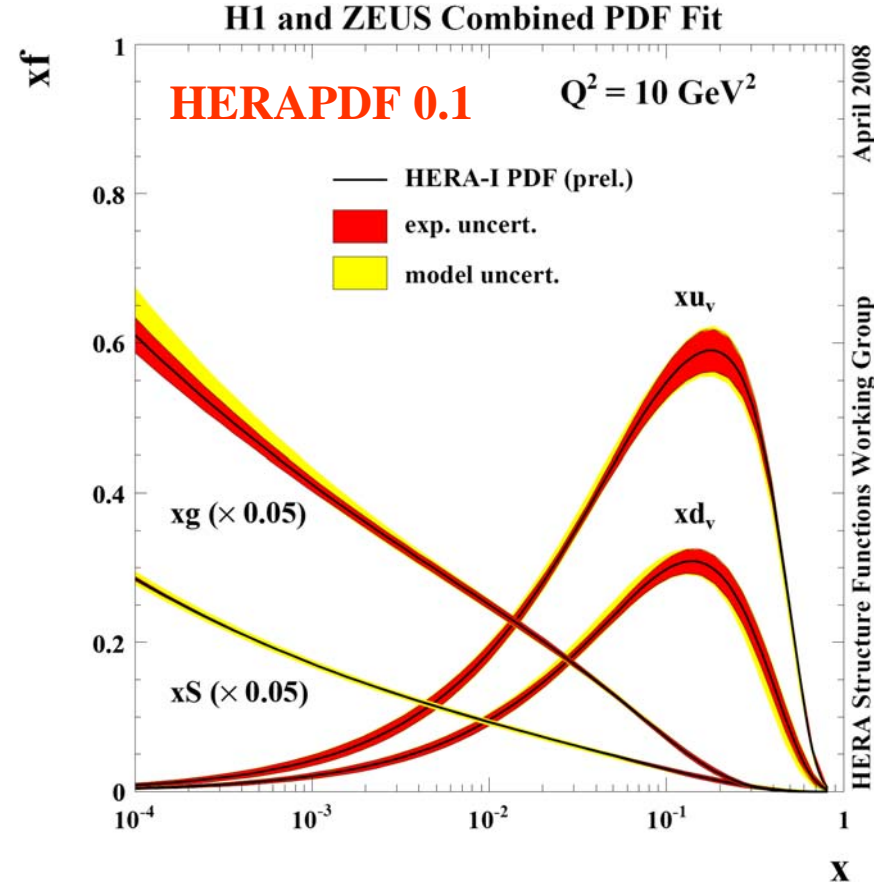
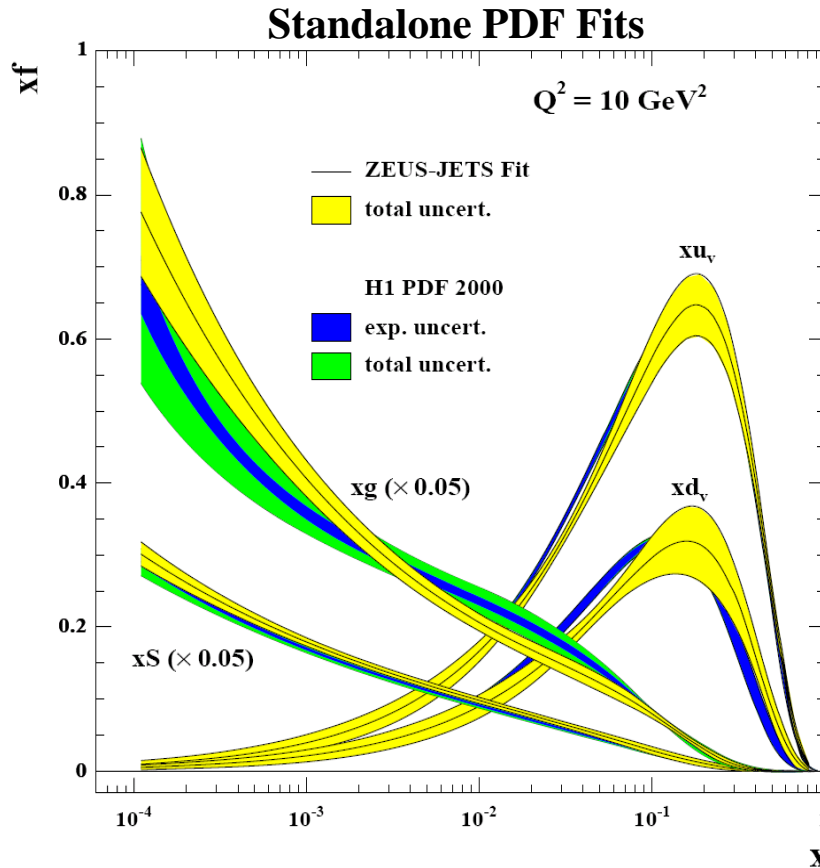
**Improved precision of σ_{CC}
By combining H1 and ZEUS**



MPI Munich

Burkard
Reisert
EINN 09
Milos

PDF Fits on HERA I Data



Impressive reduction of uncertainties of combined PDFs

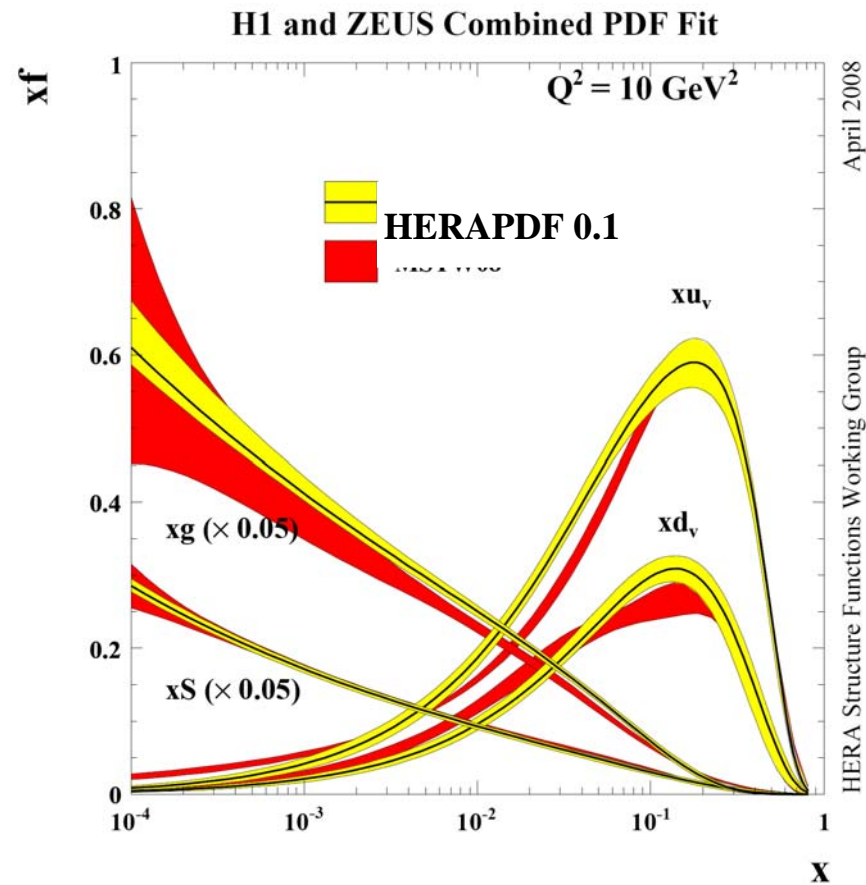
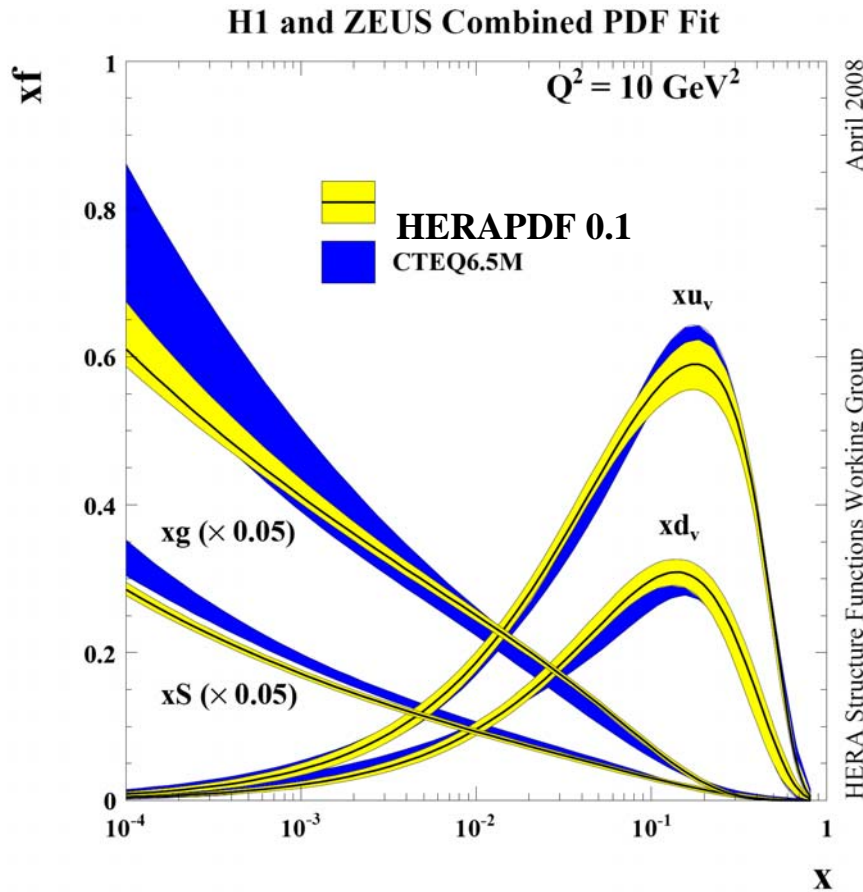
Model uncertainty: variation of charm and bottom mass, starting scale Q_0^2 , Q_{\min}^2 of included data, strange and charm fraction at starting scale



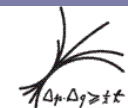
MPI Munich

Burkard
Reisert
EINN 09
Milos

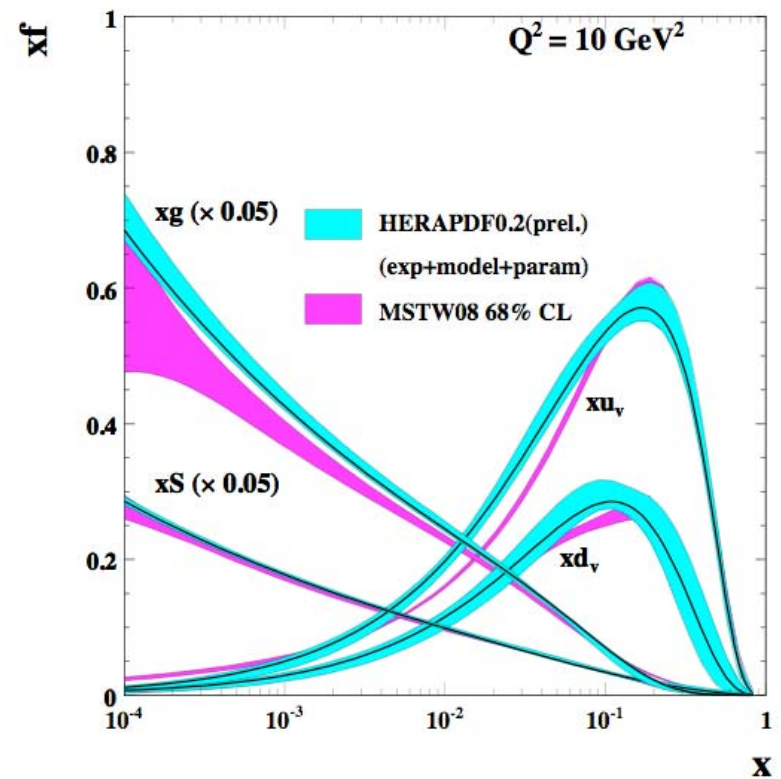
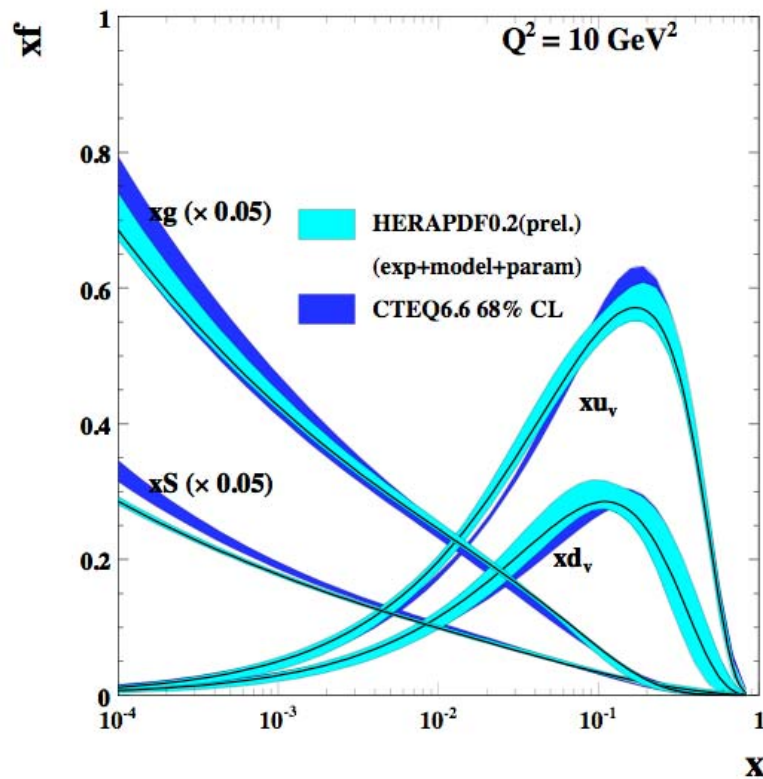
Comparison to Global Fits



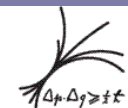
not a completely fair comparison:
HERA combined data were not available to global fitters



Comparison to Global Fits



not a completely fair comparison:
HERA combined data were not available to global fitters

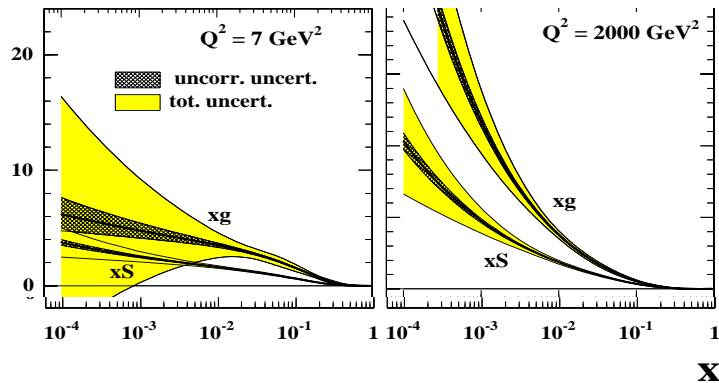


MPI Munich

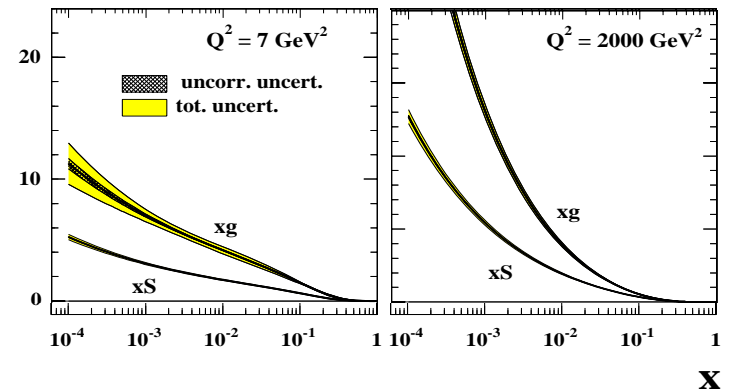
Burkard
Reisert
EINN 09
Milos

Impact of HERA data

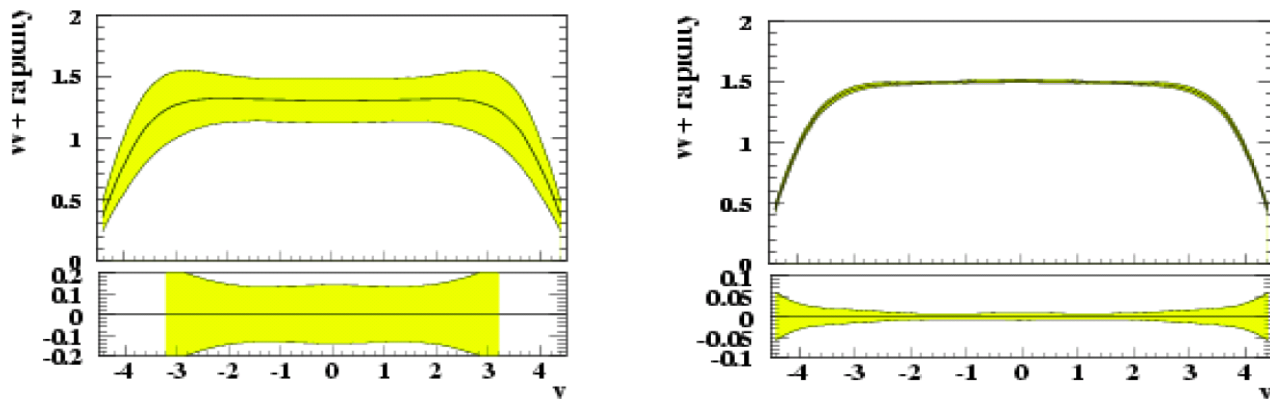
Pre-HERA uncert. in gluon/sea PDFs



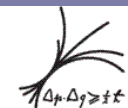
HERA PDFs combining H1 and ZEUS



Example: W^+ production at the LHC (Study by A. Cooper-Sakar)



Note: Error bands are experimental uncertainties only
model uncertainty will become increasingly important

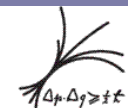


MPI Munich

Burkard
Reisert
EINN 09
Milos

Future HERA PDF Fits

- So far only part (all) of the inclusive HERA I were used → HERAPDF0.1 (0.2)
- Incorporate all NC and CC from HERA I&II
- Include jet cross sections
 - constrain high x gluon
- Include charm and beauty
 - flavor decomposition of the sea
- Charged & Neutral current cross sections with polarized e^\pm beams
 - constrain valence quark region

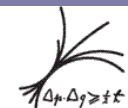
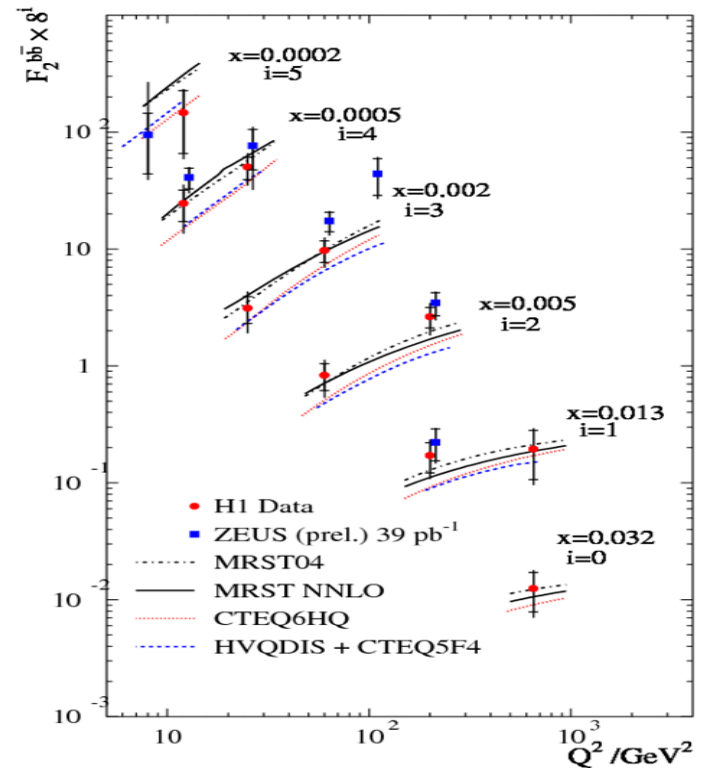
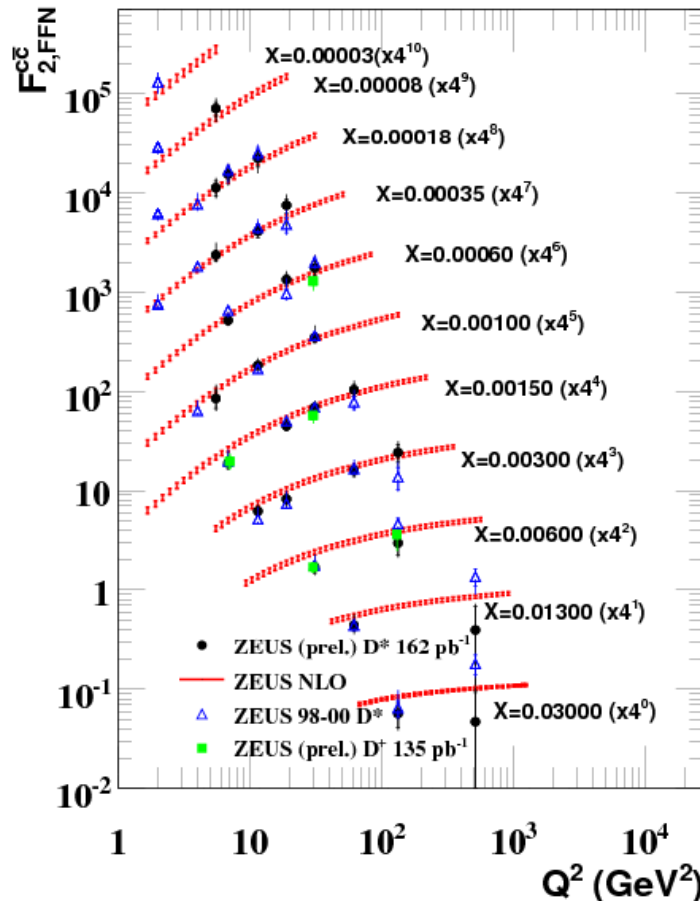
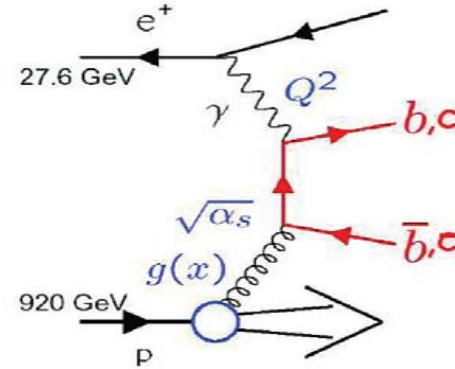


Charm & Beauty Structure

Charm and Beauty production in DIS is driven by gluons in the proton

Charm tag: reconstruct D mesons

Beauty tag: displaced vertex, soft μ



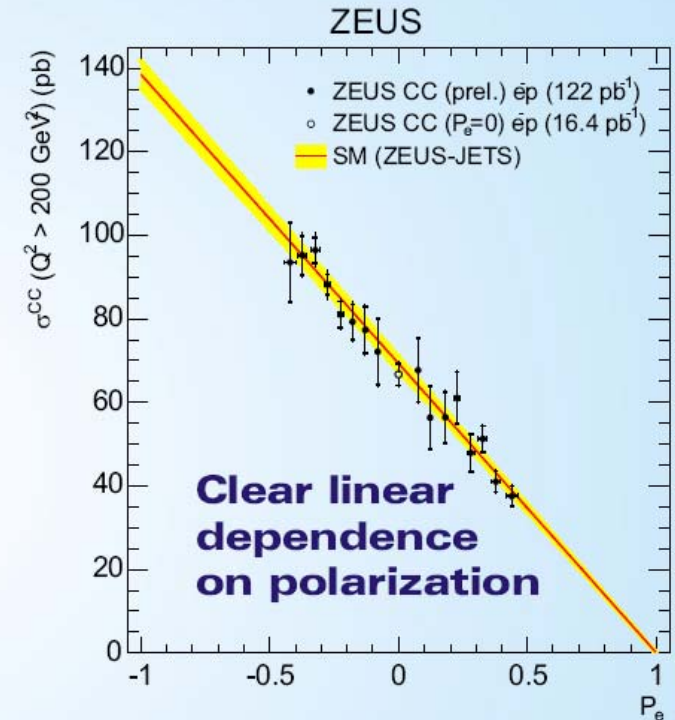
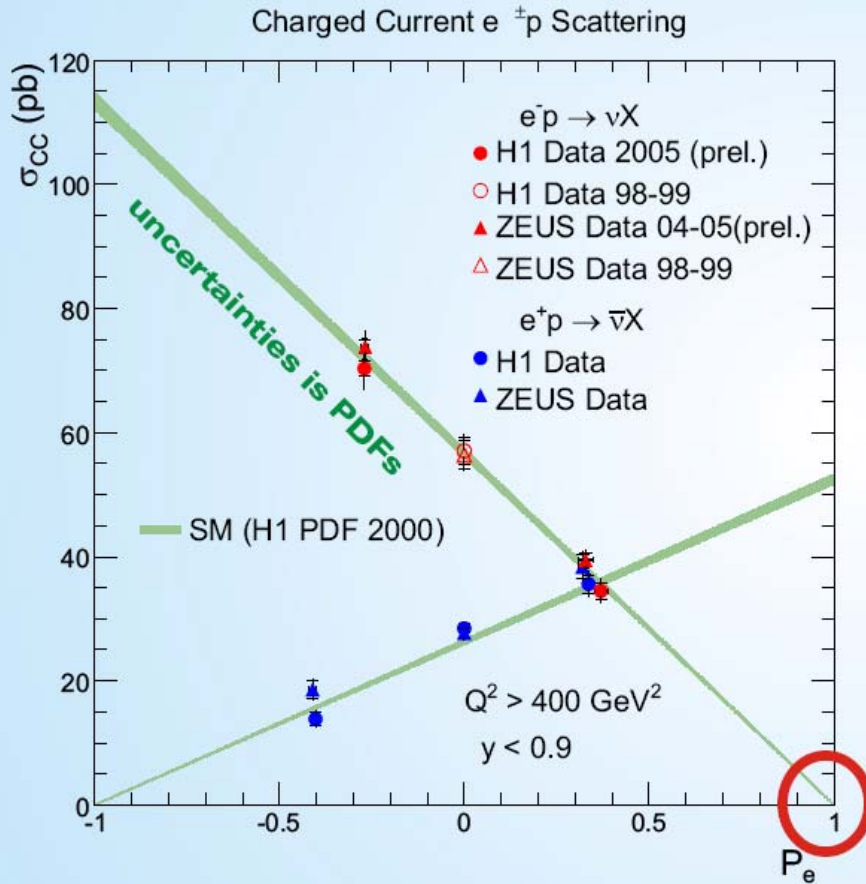
MPI Munich

Burkard
Reisert

EINN 09

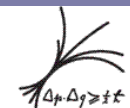
Milos

Polarization dependence of CC



Consistent with SM prediction
 $\sigma(\text{CCRH}) = 0$

Input to PDF fits: Double differential CC $e^\pm p$ cross sections



MPI Munich

Burkard Reisert

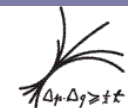
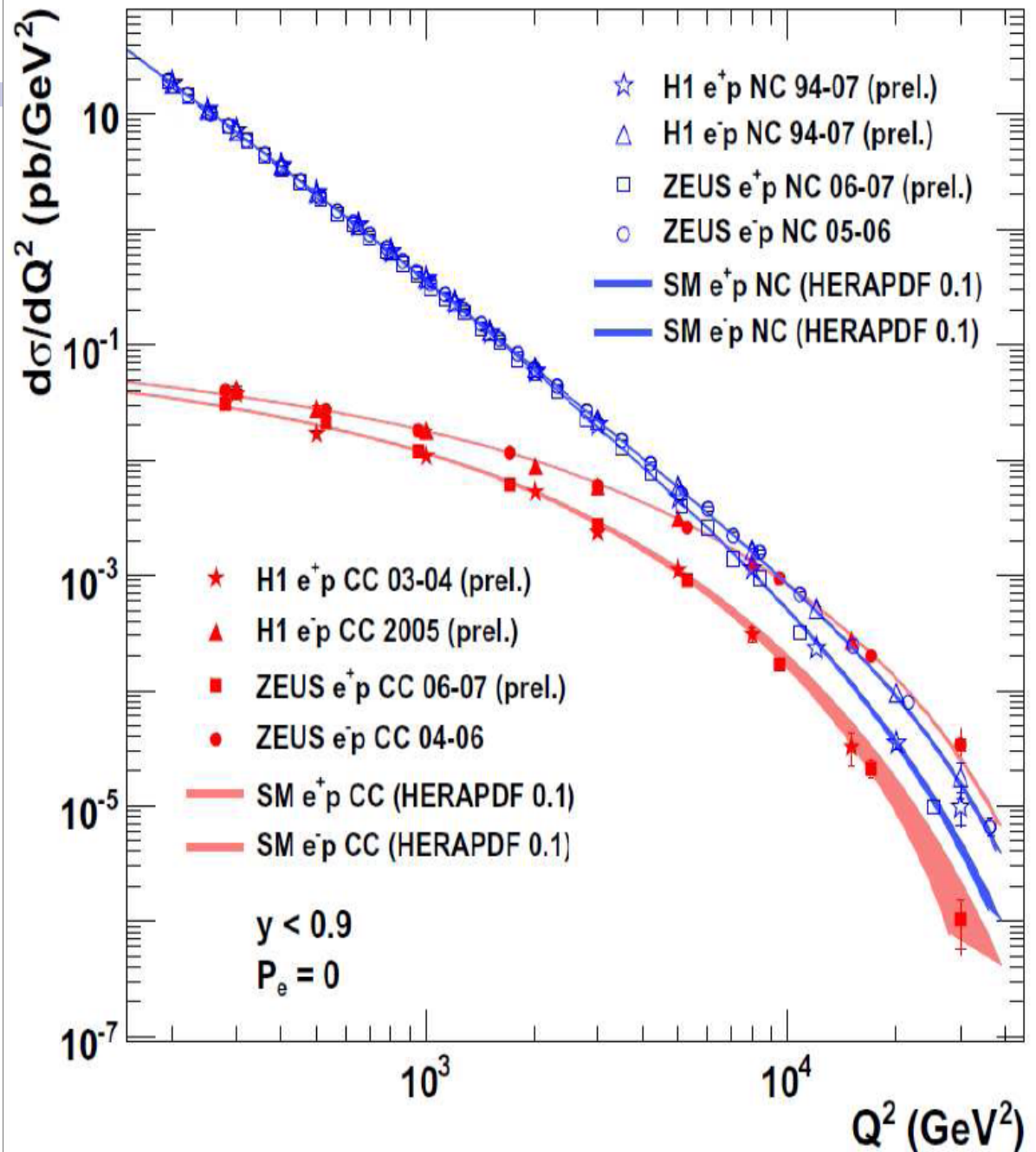
EINN 09 Milos

NC&CC

Manifestation of electroweak unification

More details on
HERA EW physics
→ see backup

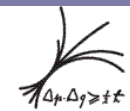
HERA I & II



MPI Munich

Burkard
Reisert
EINN 09
Milos

OPEN ISSUES



MPI Munich

Burkard
Reisert
EINN 09
Milos

Open Issues (I): high x

Inclusive cross sections at high x:

$$NC \quad e^\pm p : \sigma \propto \frac{4}{9} xu$$

$$CC \quad e^- p : \sigma \propto xu$$

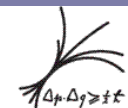
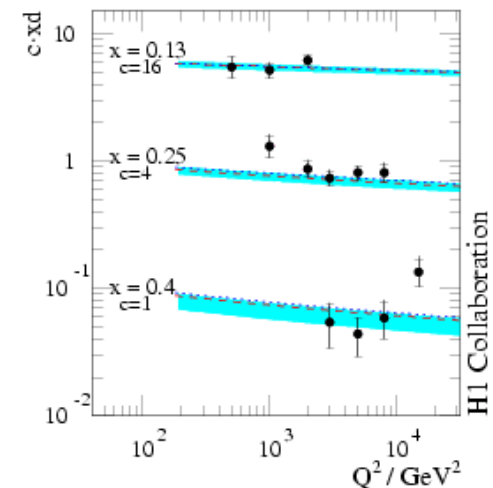
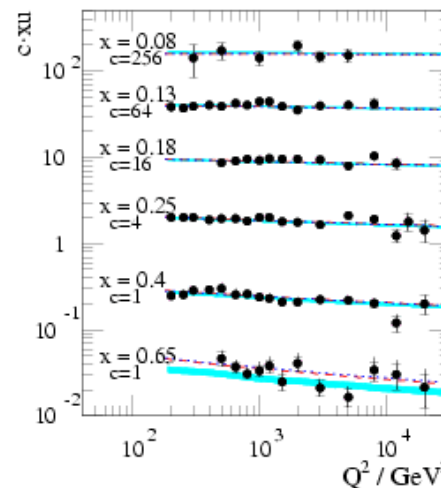
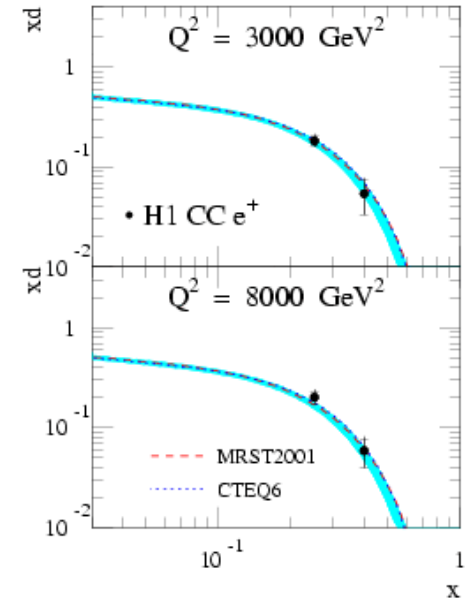
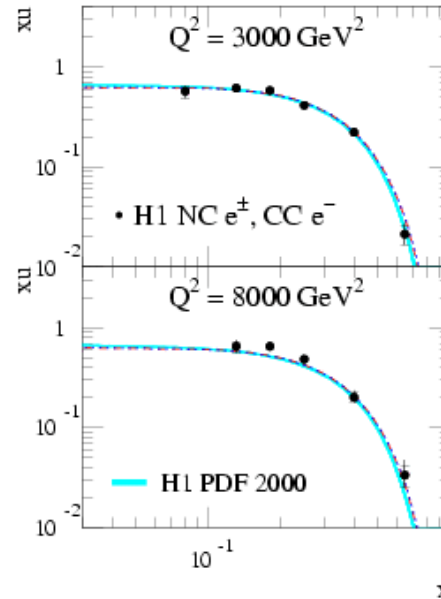
$$e^+ p : \sigma \propto (1 - y^2)xd$$

Quark distributions can be extracted with minimal corrections from QCD fits

Reach in x limited by detector acceptance, hadronic final state goes down the proton beam line

$$u: x_{\max} = 0.65$$

$$d: x_{\max} = 0.4$$



MPI Munich

Burkard
Reisert
EINN 09
Milos

Open Issues(I): High x continued

Events at high x
at acceptance limit

Poor resolution for x
→ cannot measure
differential σ at
x, Q² point

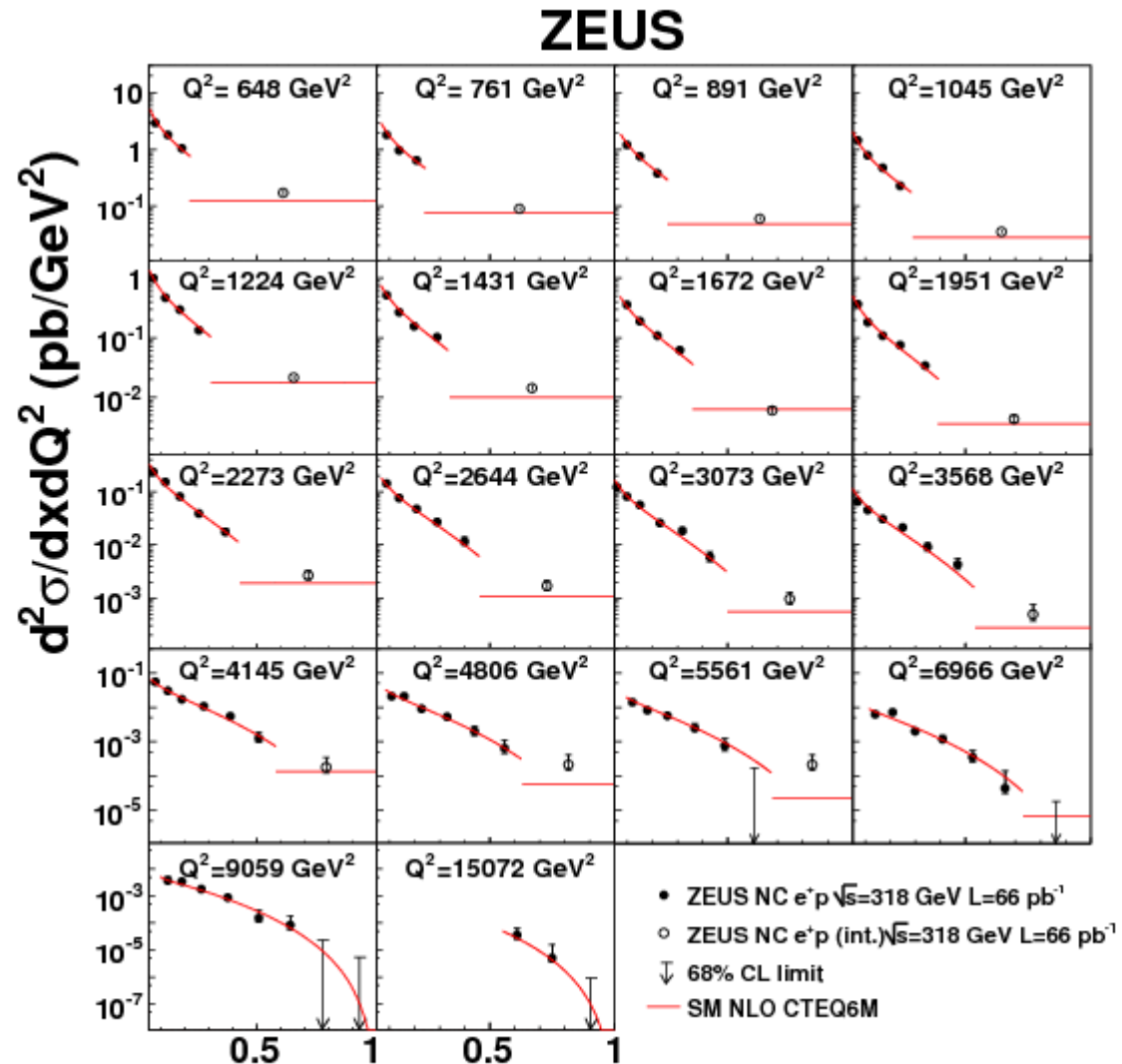
Measure integrated σ
for $x > x_{\text{limit}}$

σ larger than expected

PDFs at high x

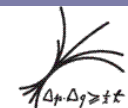
$$f \propto (1-x)^c \Rightarrow f \xrightarrow{x \rightarrow 1} 0$$

Constraint by shape
→ underestimated
uncertainty?

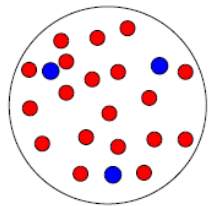
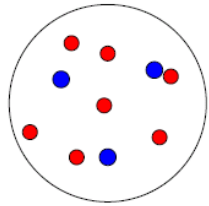
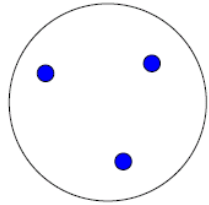


Here HERA I e^+p , e^-p see backup

X



Low x, Large Parton Densities and Saturation



at fixed resolution scale (Q^2) go to very large hadronic center of mass energy

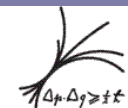
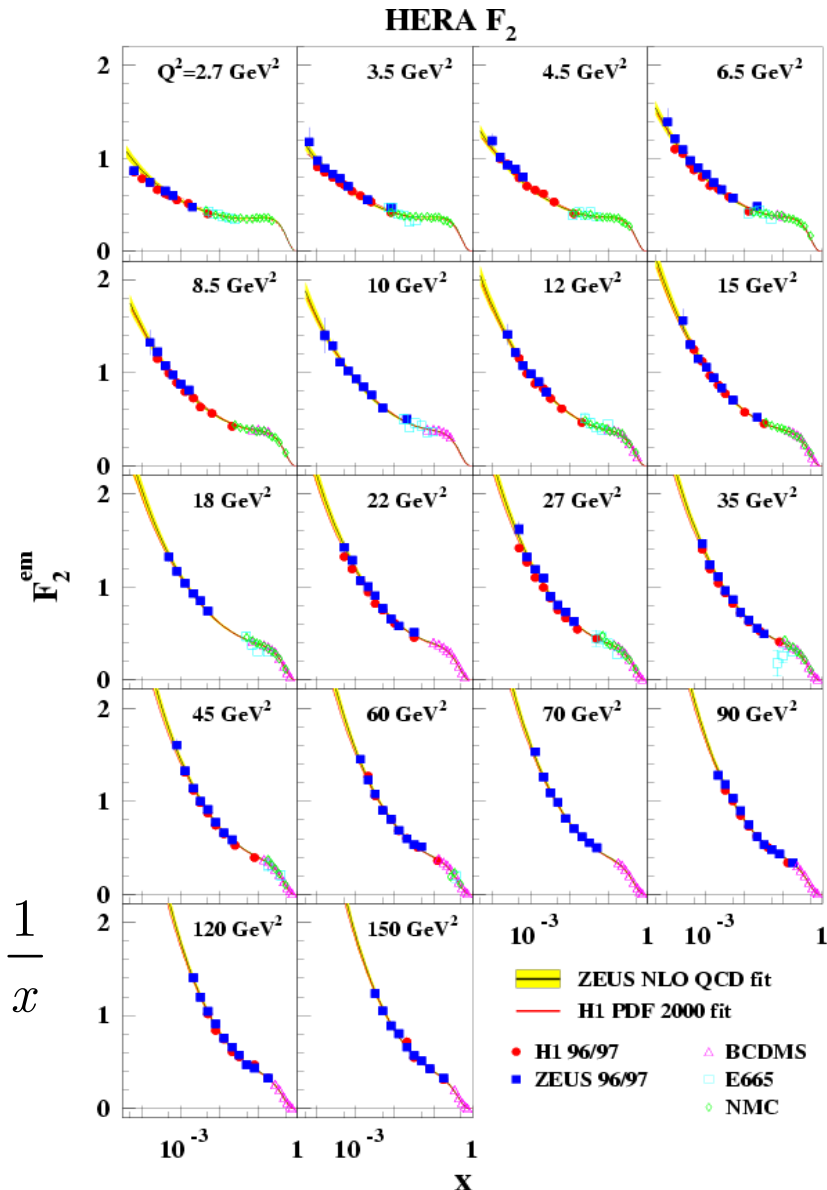
low x
$$x = \frac{Q^2}{Q^2 + W^2}$$

ultimately expect partons to overlap („saturation“)

Rise of pdf should flatten with decreasing x

$$\left(\frac{1}{x}\right)^\lambda \rightarrow \ln \frac{1}{x}$$

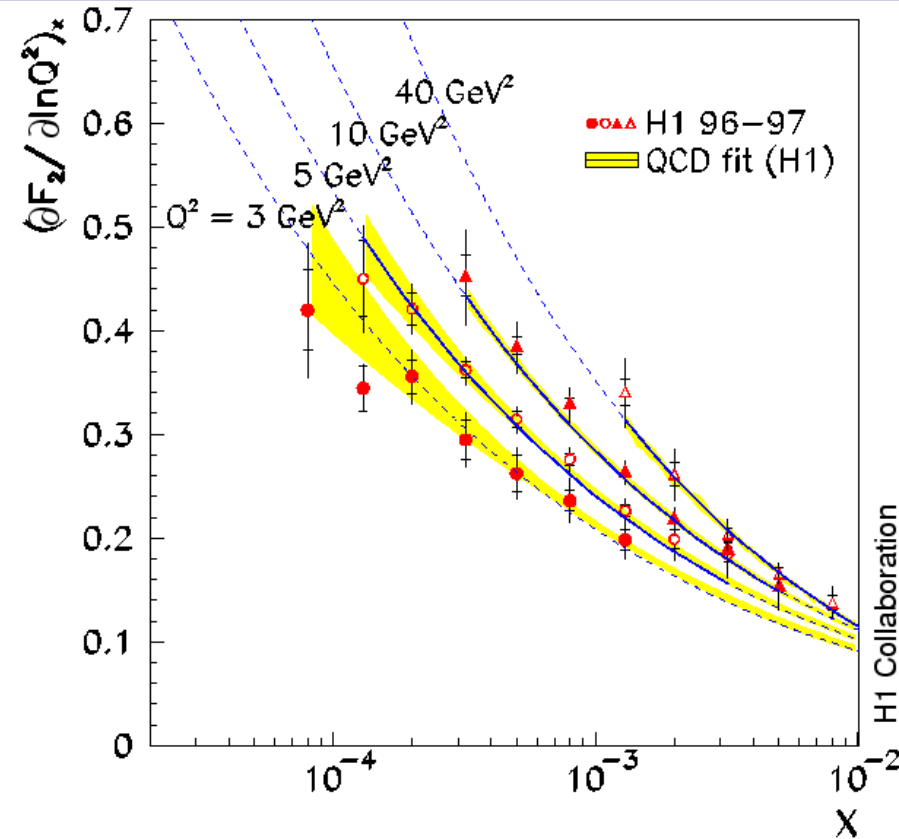
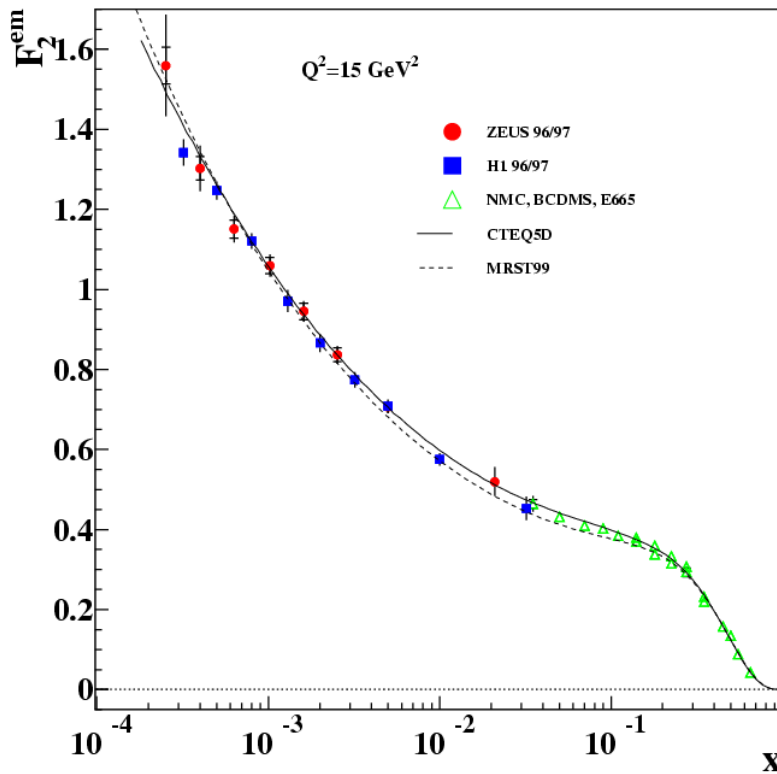
No saturation observed at HERA



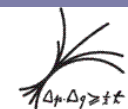
MPI Munich

Burkard Reisert
EINN 09
Milos

The Birth of Experimental Low x Physics



- Biggest HERA discovery: strong increase of quark density (F_2) and gluon density ($d F_2 / d \ln Q^2$) with decreasing x in newly explored regime.
- Low x , 'large' Q^2 is high density, low coupling limit of QCD ...
- No saturation observed yet \rightarrow probe at even smaller x



MPI Munich

Burkard
Reisert
EINN 09
Milos

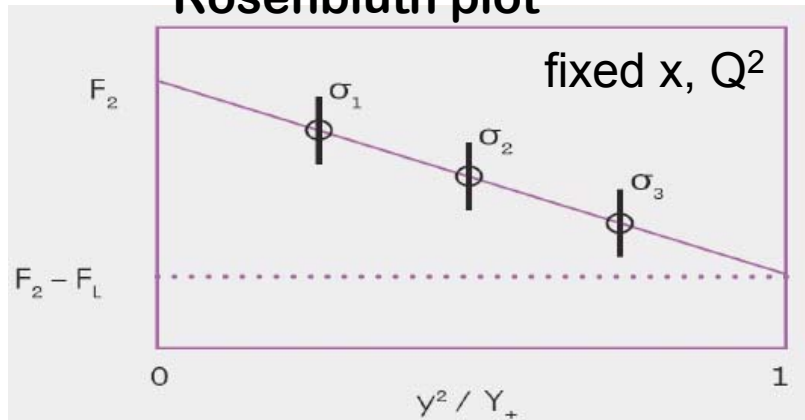
Issues at low x? Low x = High y !

- Neutral current DIS cross section expressed by structure functions:

$$\frac{d^2\sigma^{e^\pm p \rightarrow e^\pm X}}{dx dQ^2} = \frac{2\pi\alpha^2}{xQ^4} \underbrace{\left(1 + (1-y)^2\right)}_{Y_\pm = 1 \pm (1-y)^2} \cdot \left(F_2(x, Q^2) - \frac{y^2}{Y_+} F_L(x, Q^2) \right)$$

$\tilde{\sigma}$: Reduced cross section

Rosenbluth plot



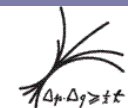
$$F_2(x, Q^2) = \sigma_r(x, Q^2, y=0)$$

$$F_L(x, Q^2) = - \frac{\partial \sigma_r(x, Q^2, y)}{\partial (y^2 / Y_+)}$$

Measure σ_r at fixed x, Q^2 but varying y

$$y = Q^2 / sx \quad \sqrt{s} = ep \text{ center-of-mass energy}$$

Varying $y \rightarrow$ varying $s \rightarrow$ dedicated low E_p runs at end of HERA



MPI Munich

Burkard
Reisert

EINN 09

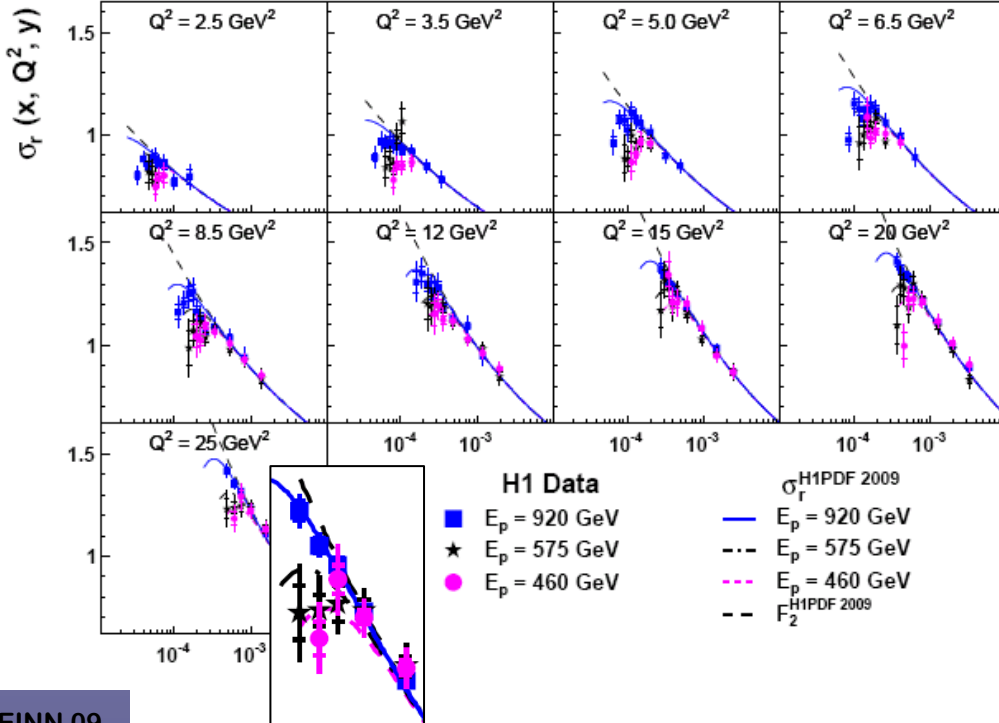
Milos

Cross Sections for direct FL extraction

Direct F_L measurement requires measurement of the reduced cross sections at **same x and Q^2 but different y** :

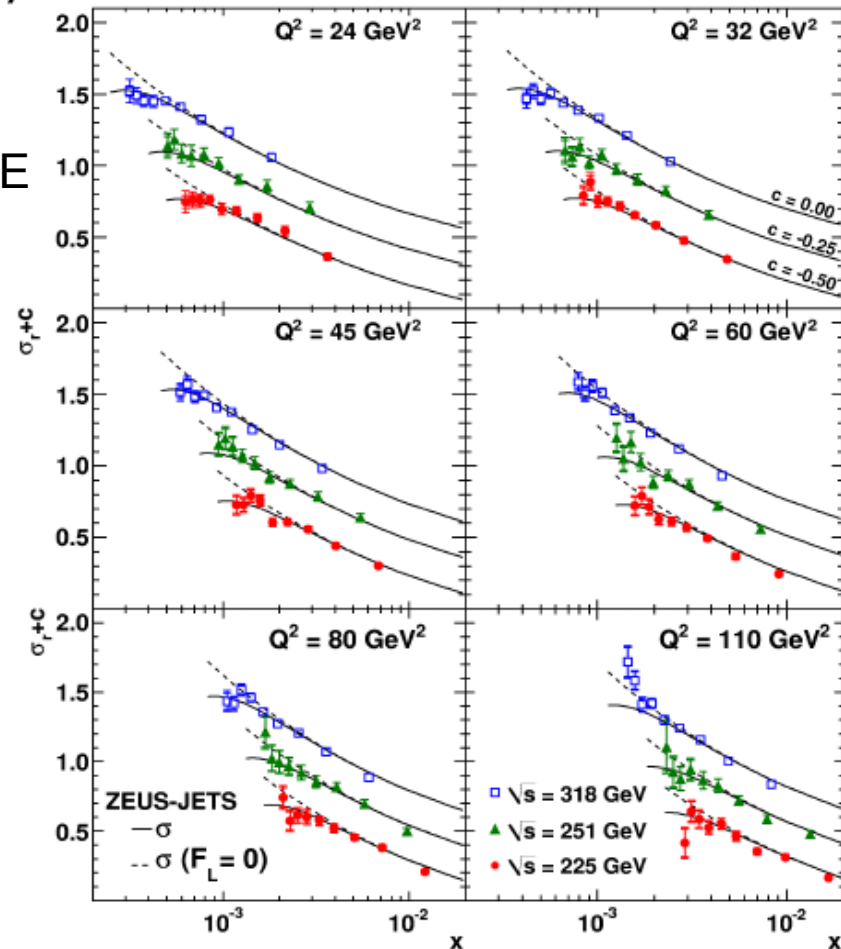
$$\sigma_r(x, Q^2, y) = F_2(x, Q^2) - \frac{y^2}{Y_+} \cdot F_L(x, Q^2)$$

$$y = \frac{Q^2}{x \cdot s} \quad \text{different } y \rightarrow \text{different } s \rightarrow \text{different beam energy}$$



Turnover due to F_L small but visible

ZEUS



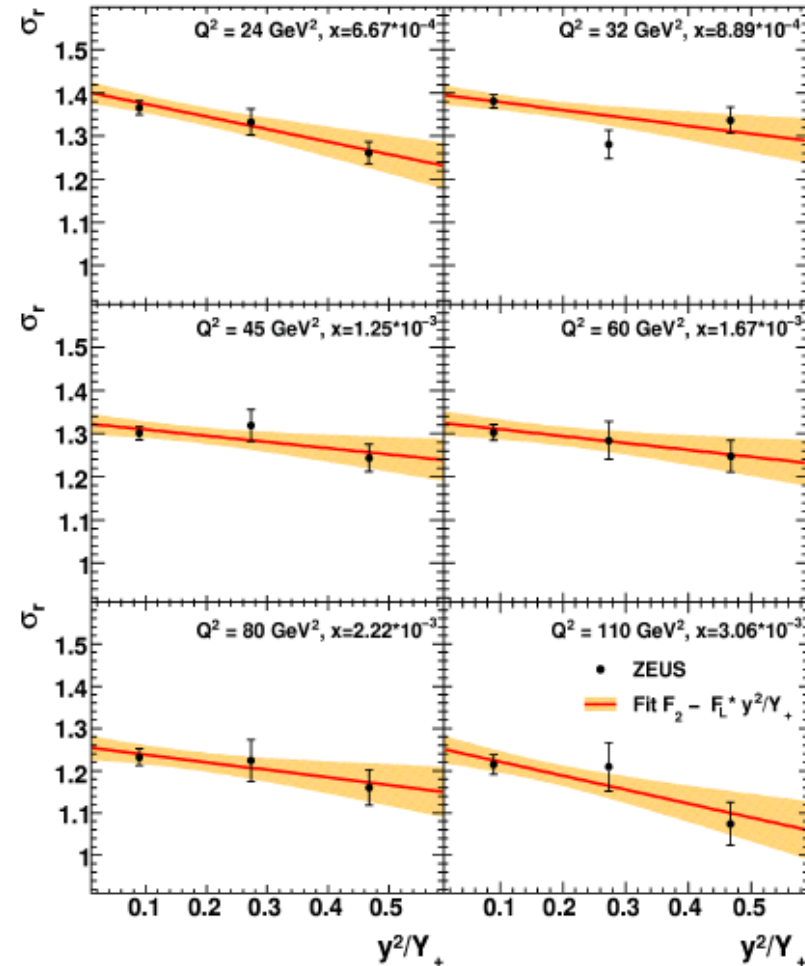
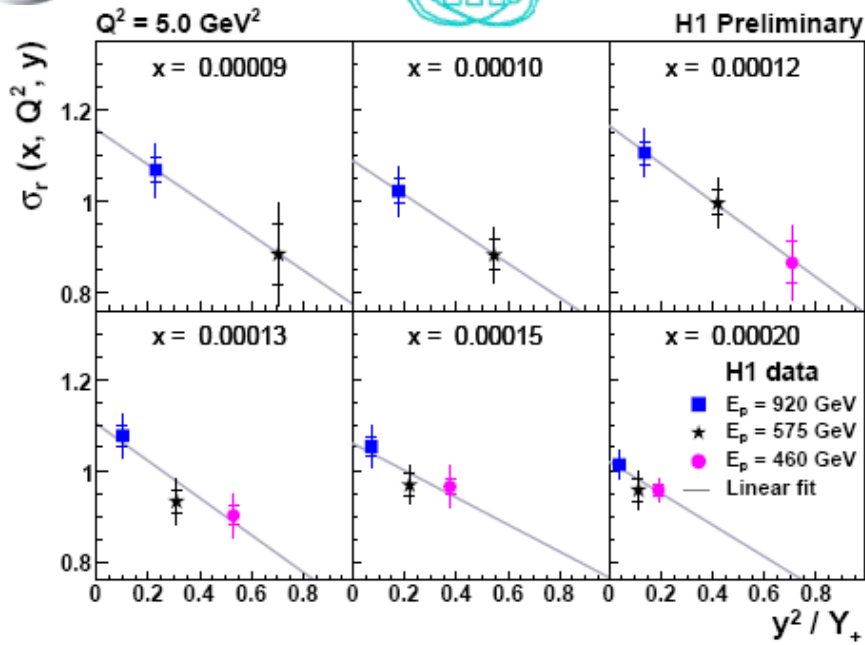
most precise σ_r from ZEUS

F_L Extraction: Rosenbluth plots

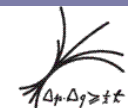
$$\sigma_r(x, Q^2, y) = F_2(x, Q^2) - \frac{y^2}{Y_+} \cdot F_L(x, Q^2)$$

Straight line fit of σ_r vs y^2/Y_+
 F_L slope, F_2 intercept

ZEUS



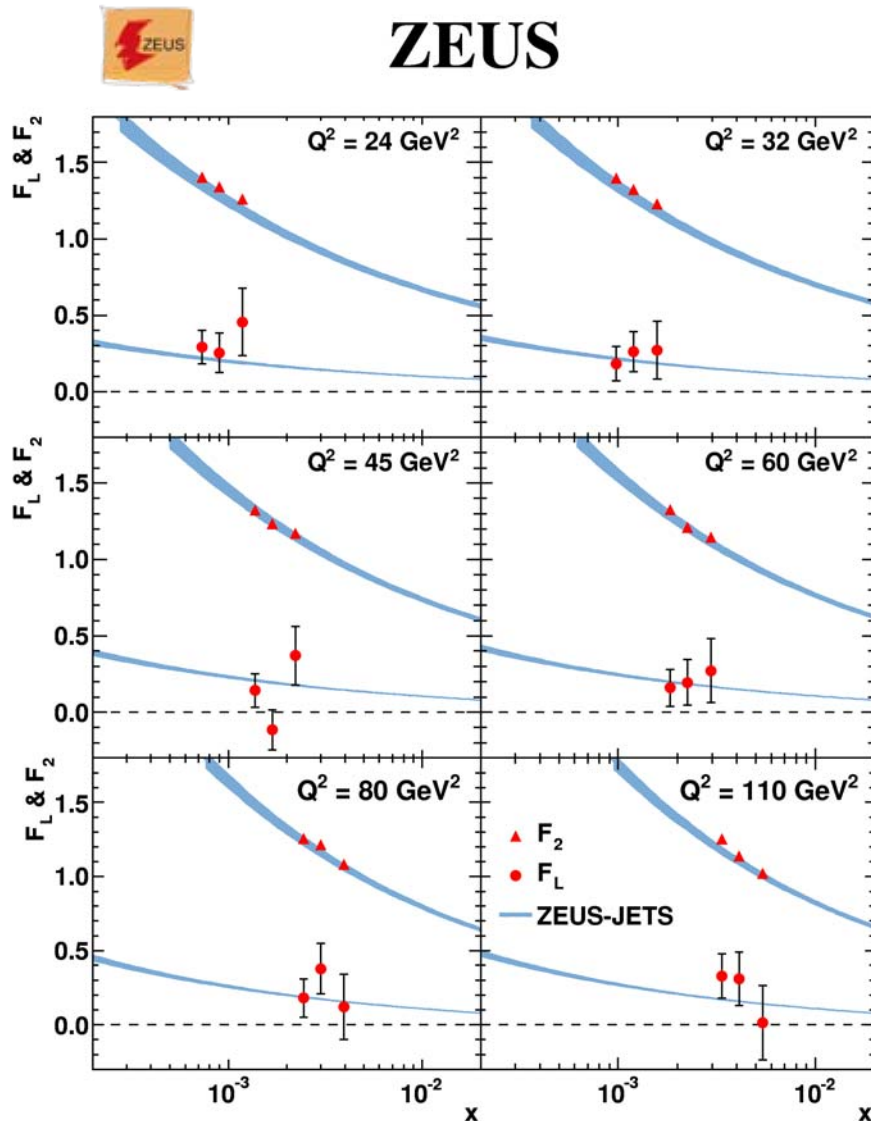
Full information of correlated systematics taken into account ₂₈



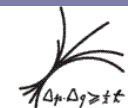
MPI Munich

Burkard
 Reisert
 EINN 09
 Milos

Extracted F_L and F_2 – ZEUS



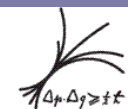
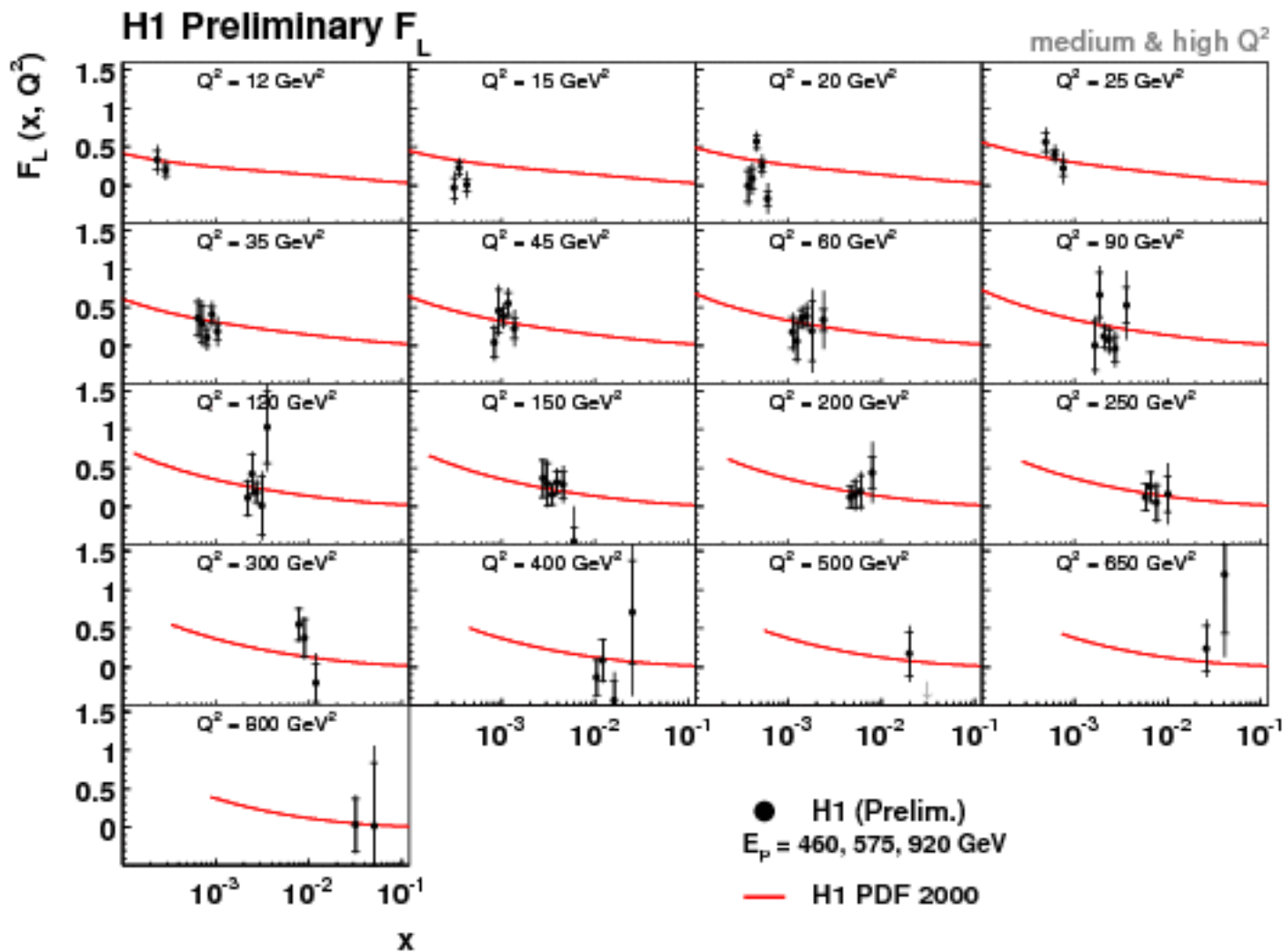
- Most precise F_2 measurement from ZEUS in kinematic region studied
- First F_2 measurement without assumptions on F_L
- Data support a non-zero F_L
- Predictions for F_2 and F_L are consistent with data



MPI Munich

Burkard
Reisert
EINN 09
Milos

Extracted F_L – medium & high Q^2

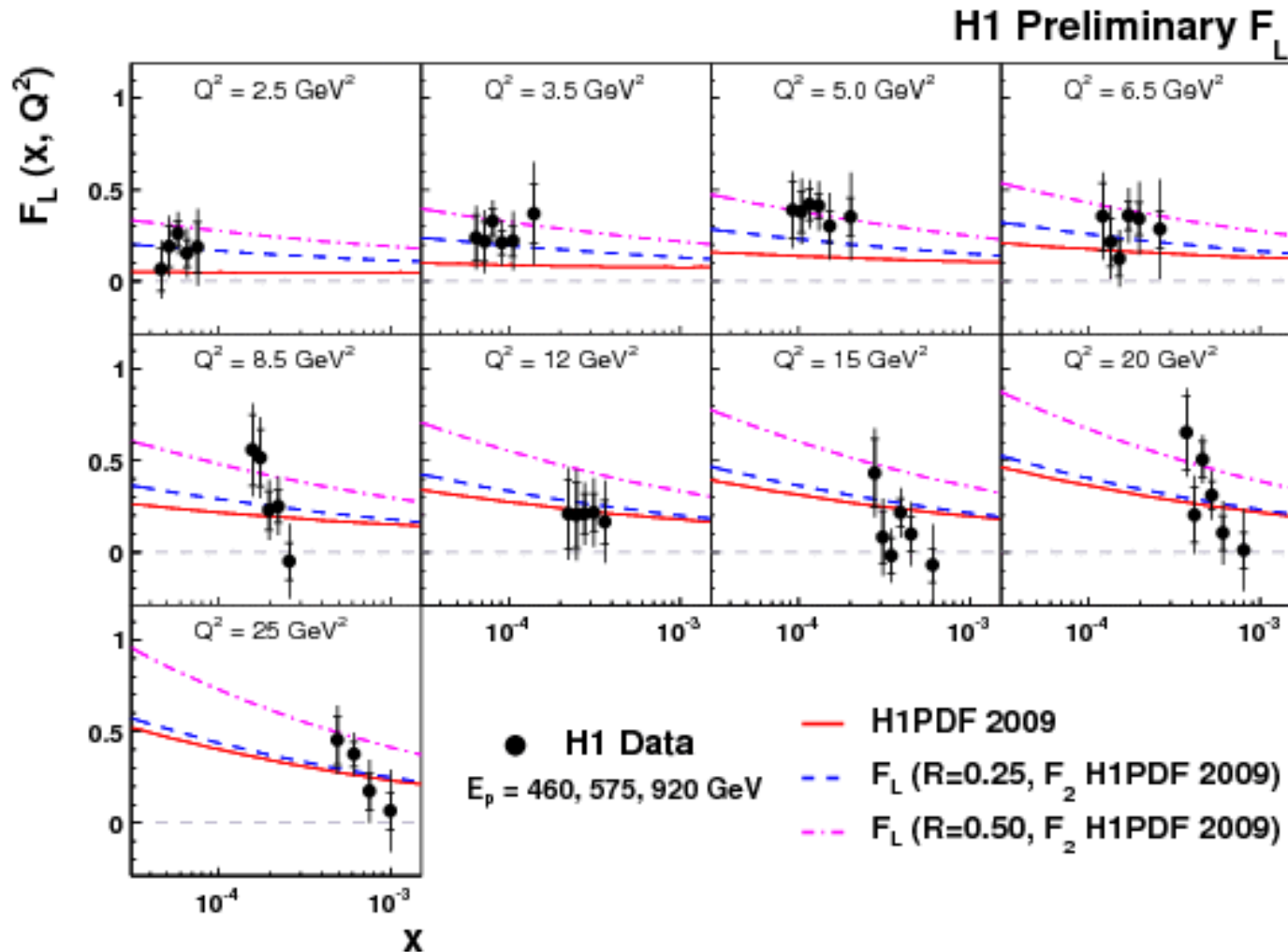


MPI Munich

Burkard
 Reisert
 EINN 09
 Milos

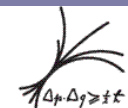
Medium Q^2 published in Phys. Lett. B665, p. 139

Extracted F_L – Low Q^2



F_L measured down to $Q^2 = 2.5 \text{ GeV}^2$!

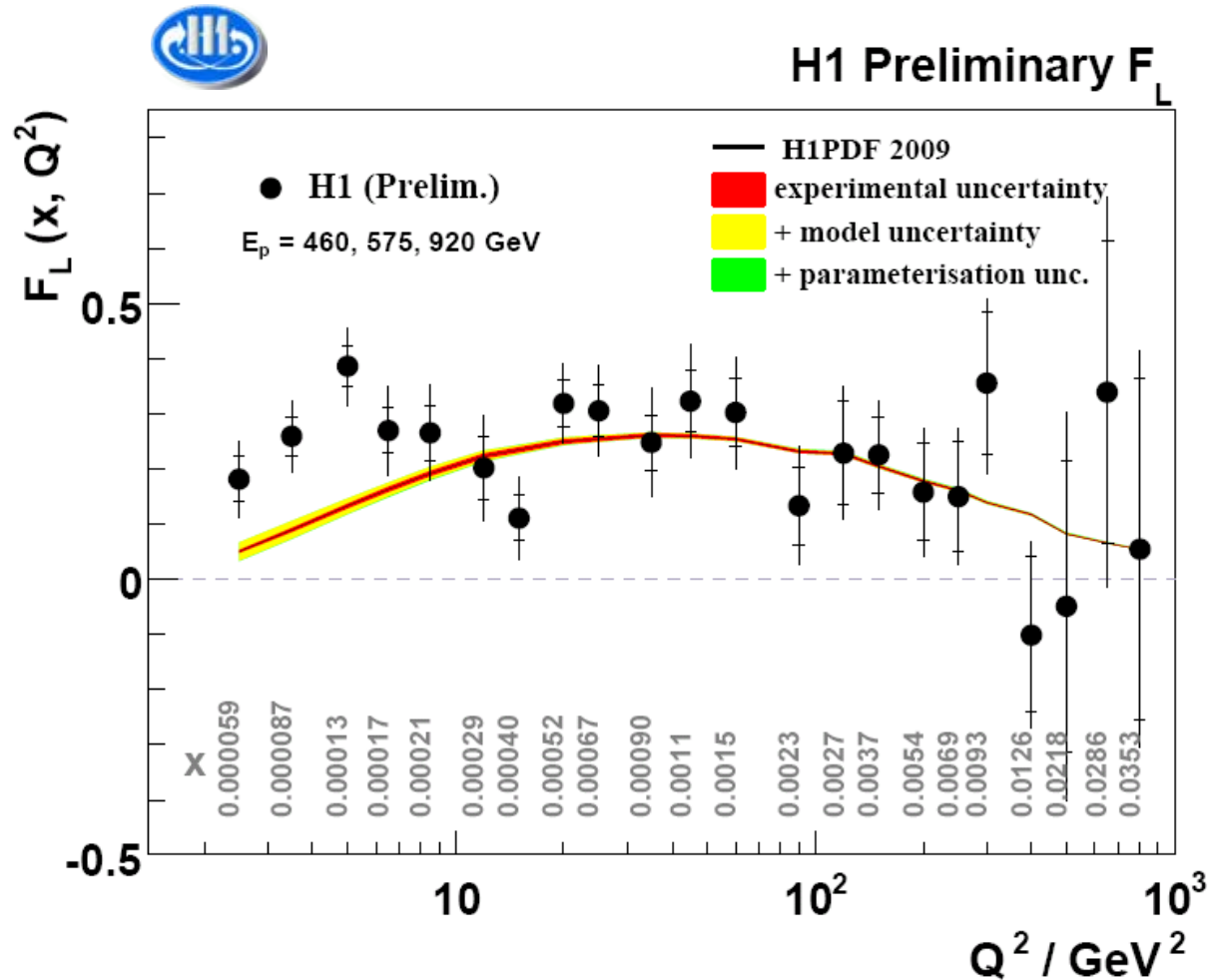
Data are consistent with $R \sim 0.25$ ($F_L = 0.2 \cdot F_2$)



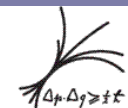
MPI Munich

Burkard
Reisert
EINN 09
Milos

Average F_L – H1



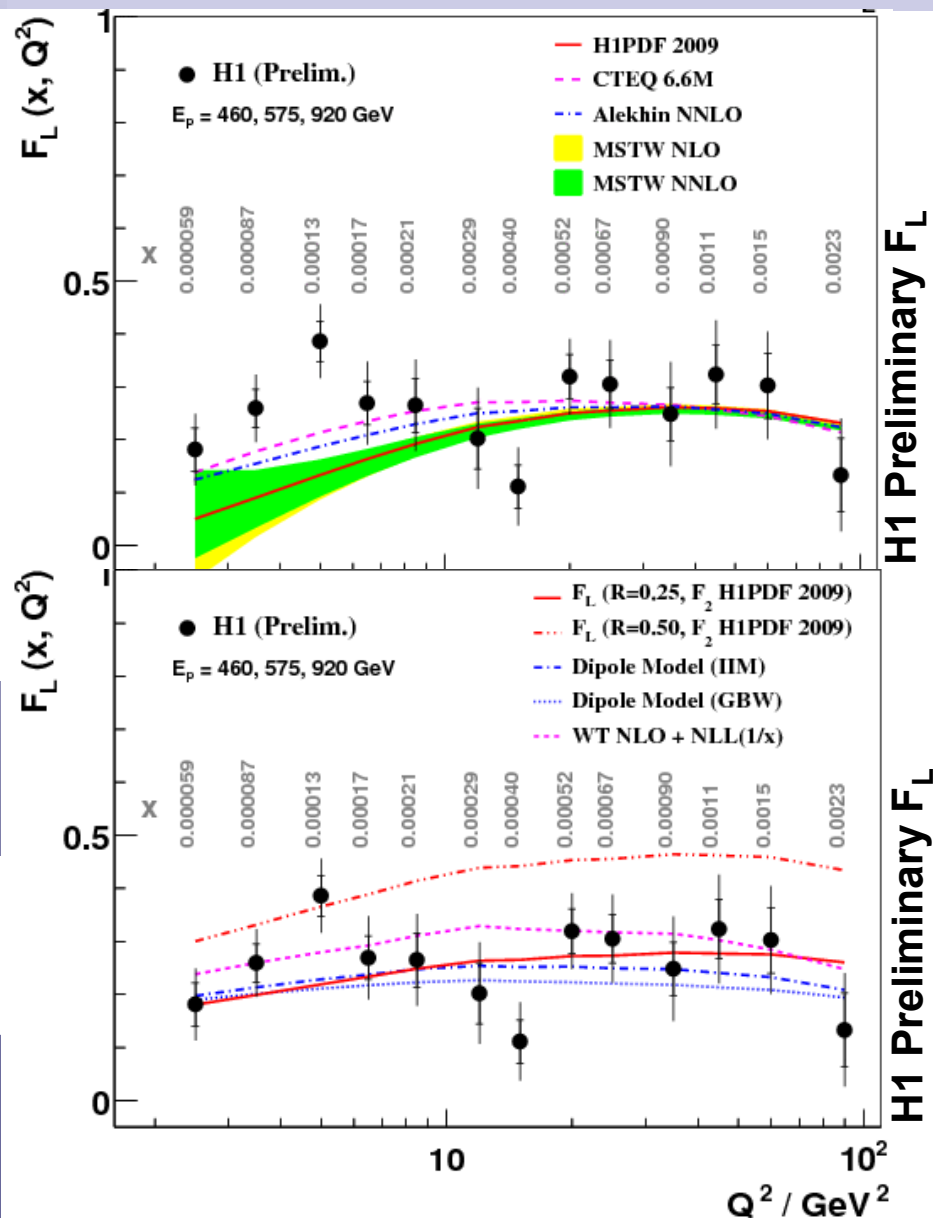
H1 measurements cover $2.5 \leq Q^2 \leq 800 \text{ GeV}^2$ and $0.00005 \leq x \leq 0.05$
 For $Q^2 \geq 10 \text{ GeV}^2$, agree well with H1PDF 2009 prediction.



MPI Munich

Burkard
 Reisert
 EINN 09
 Milos

Average $F_L < 100 \text{ GeV}^2$

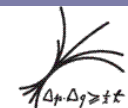


- MSTW and H1PDF 2009 predictions use the same heavy flavour scheme to calculate F_L .

- Data agree better with calculation of CTEQ (and Alekhin)

- Data is consistent with constant $R \sim 0.25$ (H1)
- $R = 0.18^{+0.07}_{-0.05}$ (ZEUS).
- $R = F_L / (F_2 - F_L)$

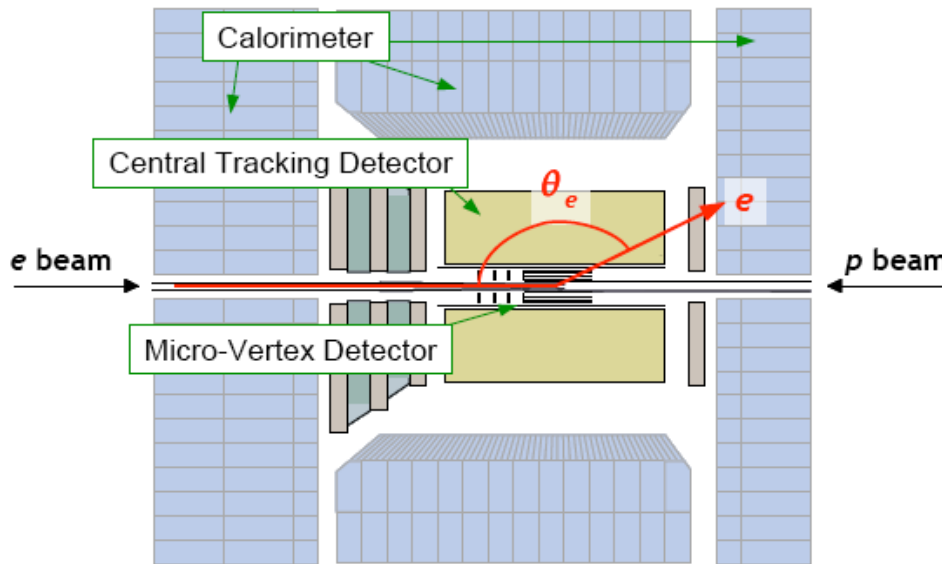
- Good agreement with IIM and GBW dipole models, NLL(1/x) prediction.



MPI Munich

Burkard
Reisert
EINN 09
Milos

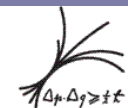
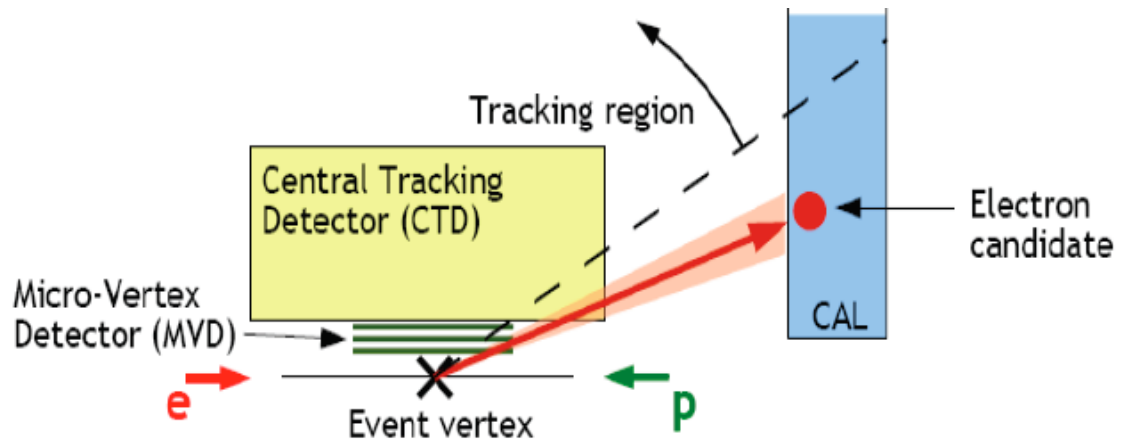
Measuring FL with ZEUS



Event Selection:

- Electron in backward Calo
- $E'_e > 6$ GeV (Cluster & Trigger)
- Hits in CTD & MVD (reject neutrals)
- Event vertex
- $42 < E-p_z < 65$ GeV

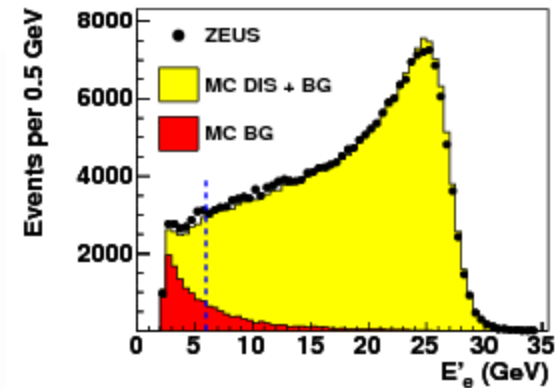
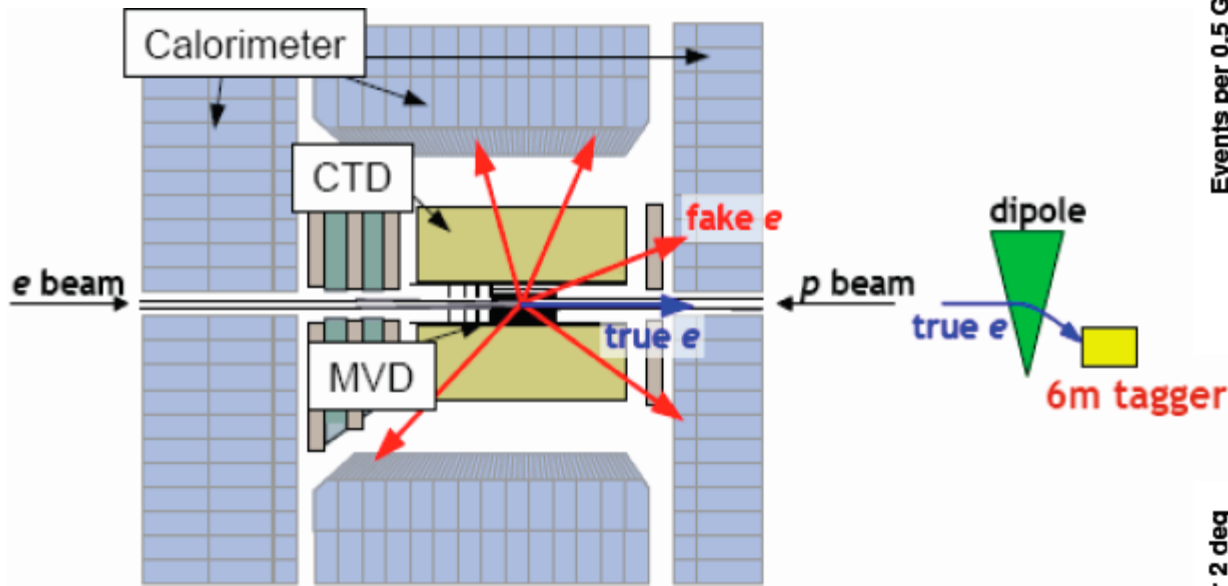
Q^2 range between
24 and 110 GeV²



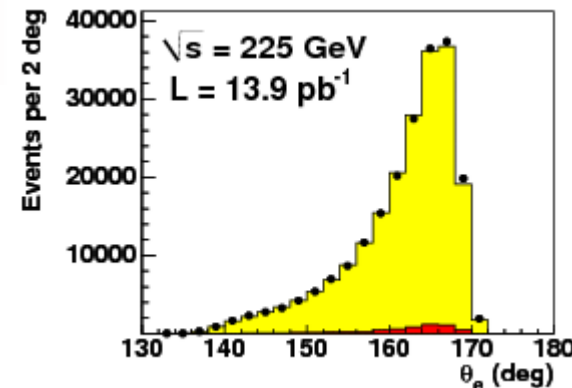
MPI Munich

Burkard
Reisert
EINN 09
Milos

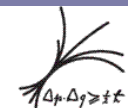
Background Subtraction - ZEUS



ZEUS



Photoproduction BG removed using PYTHIA MC with subprocesses (direct, resolved, diffractive,...) weights Adjusted to γp cross section measurement.
Control using 6m electron tagger. Complimentary studies with γp enriched data sample.

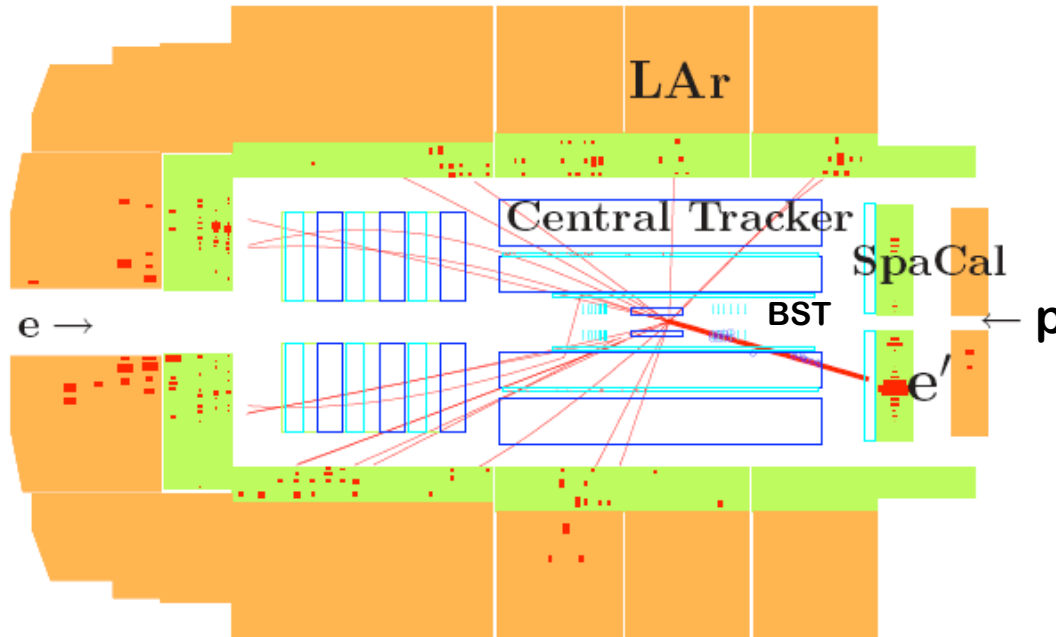


MPI Munich

Burkard
Reisert
EINN 09
Milos

Measuring F_L with H1

DIS event of Q^2 near 30 GeV^2



Upgrades for FL

SpaCal (94)

BST (95+03)

Triggers (03-07)

- Inner Chamber (CIP)
- SpaCal
- Fast Tracking (CJC)
- Jet Trigger (LAr)

Three Q^2 ranges

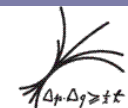
3 to 12 GeV^2 SpaCal+BST
prelim. 04/09

12 to 90 GeV^2 SpaCal+CT:
published 08

35 to 800 GeV^2 LAr+CT:
prelim. 03/08

Event selection Criteria

- El. in SpaCal or LAr (Calo & Trig) $E'_e > 3 \text{ GeV}$
- Track in CT or BST (veto neutrals, e/p)
- Interaction vertex
- $E-P_z = \sum_i E_i (1 - \cos \theta_i) > 35 \text{ GeV}$
- Reduces largely radiative corrections



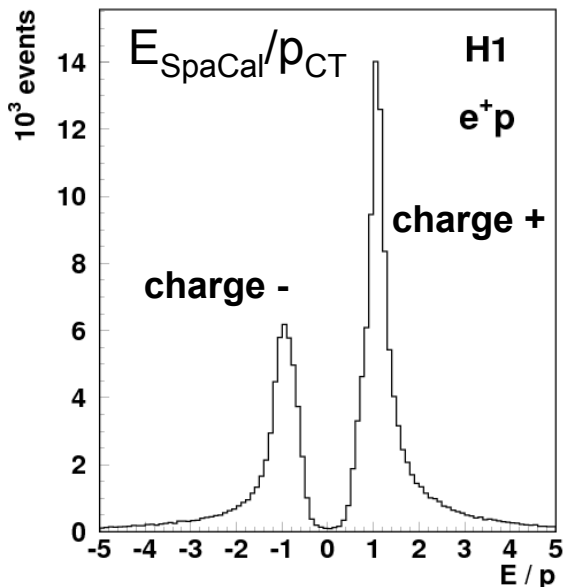
MPI Munich

Burkard
Reisert
EINN 09
Milos

Background Subtraction – H1

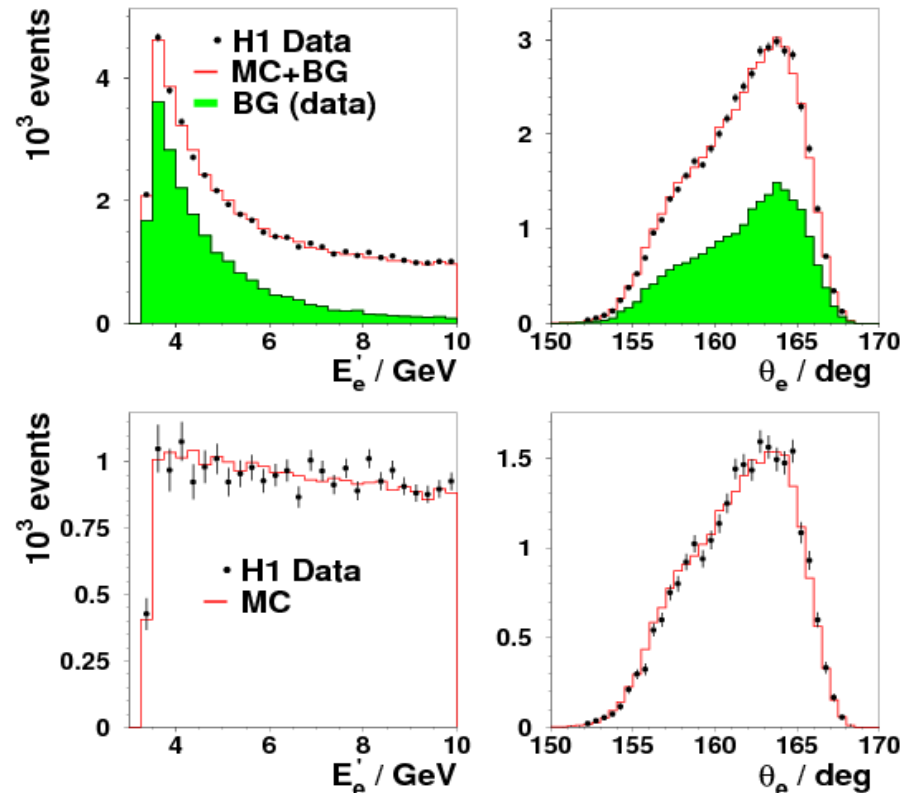
At small energies severe contamination by γp events.

Those are charge symmetric, apart from small effects due to anti-proton vs protons, which is measured using e^+p and e^-p data, and corrected for

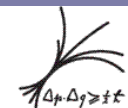


H1 has tracking coverage for the electron candidates for all full Q2 ranges (CT & BST)

Scattered electron distributions (SpaCal + CT)



H1 background subtraction based on data. Trade off between background rejection and stat. unc. of background sample (wrong chrg.)



Summary

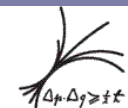
Precision measurements from HERA

- inclusive NC & CC cross sections
- structure functions
- parton densities

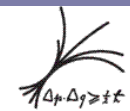
Many more not shown:
QCD-Jets, Diffraction,
Exclusive vector mesons,
DVCS, searches BSM limits ...

Issues:

- **valence quarks** constrained by NC & CC at high Q^2
 d_v will remain less precise than u_v
- **sea quarks** obtained from F_2 at low x
possibility of an asymmetric light flavor sea $\bar{d}-\bar{u}\neq 0$
- **gluons** from scaling violations, F_L , jets, vector mesons, $c\bar{c}$ $b\bar{b}$
ultimately precision to be seen, final uncertainty at high x ?
- **high x** : extrapolating towards $x\rightarrow 1$
How to assess uncertainties?
- **low x** : When does the strong rise saturate?



Backup Slides



MPI Munich

Burkard
Reisert
EINN 09
Milos

Polarisation Effects in NC

$$\begin{aligned}\tilde{F}_2 &= F_2^\gamma - (v_e \pm P_e a_e) \chi_Z F_2^{\gamma Z} + ((v_e^2 + a_e^2) \pm P_e 2v_e a_e) \chi_Z^2 F_2^Z \\ \tilde{F}_3 &= - (a_e \pm P_e v_e) \chi_Z F_3^{\gamma Z} + ((2v_e a_e \pm P_e (v_e^2 + a_e^2)) \chi_Z^2 F_3^Z\end{aligned}$$

Nb.: χF_3 is written as F_3 for simplicity

- Polarization modifies γZ and Z terms:

- Axial in F_2 , vector in F_3
- dependent on size of P_e

$$u_e \approx 0$$

- F_2 : 1st order, $\sim \pm P_e a_e \chi_Z F_2^{\gamma Z}$
- F_3 : 2nd order only, $\sim \pm P_e a_e^2 \chi_Z^2 F_3^Z$

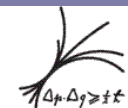
Unpol:

$$\sigma(e^+) - \sigma(e^-) \rightarrow F_3^{\gamma Z}$$

Pol :

$$\sigma(P_e \rightarrow) - \sigma(P_e \leftarrow) \rightarrow F_2^{\gamma Z}$$

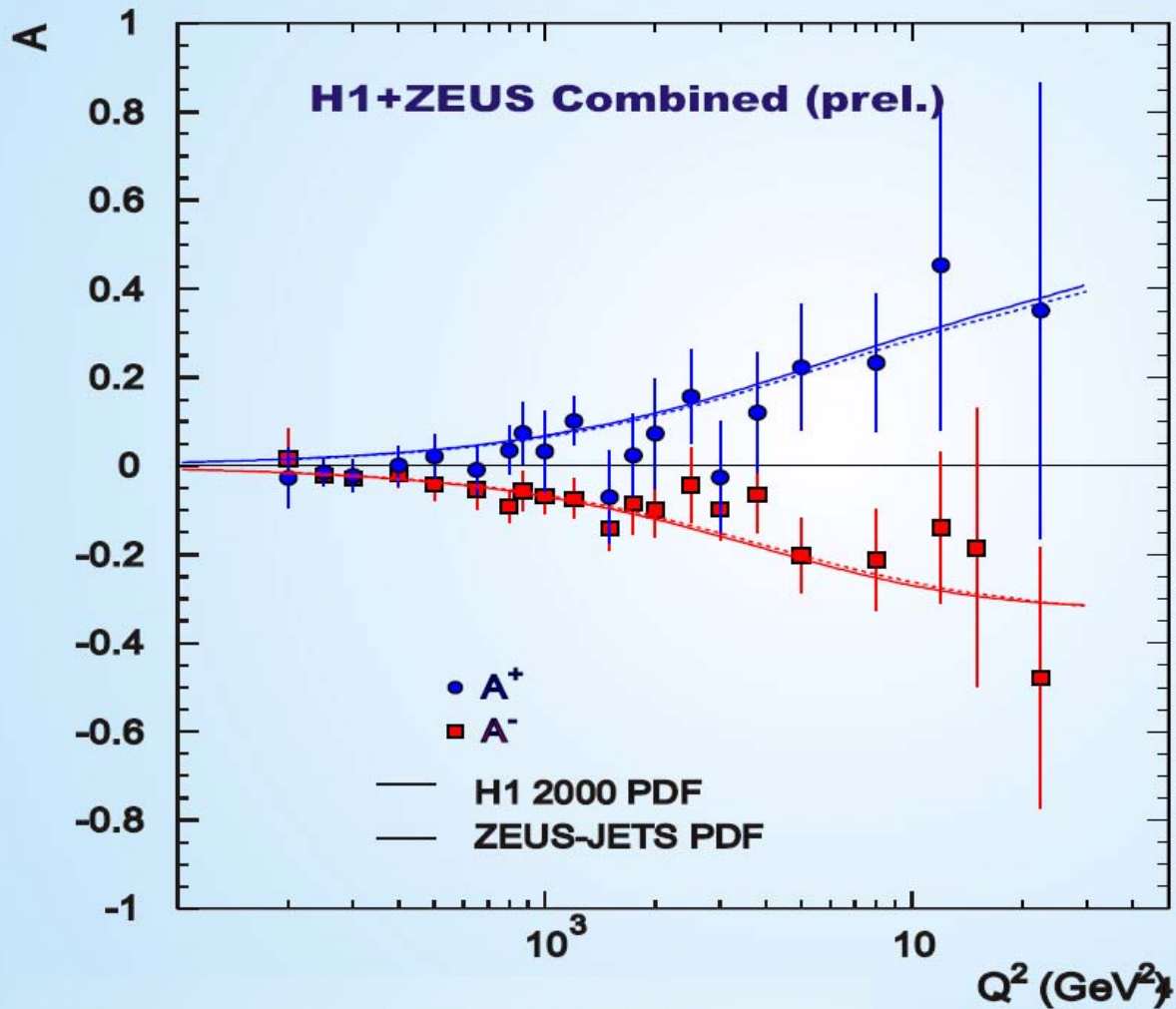
- Polarization effects expected only at EW scale, i.e large Q^2



MPI Munich

Burkard
Reisert
EINN 09
Milos

NC Cross Section Asymmetries



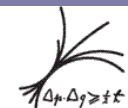
**Parity Violation
 due to γZ
 interference**

**At high x ,
 assuming
 SM couplings**

$$A_{\pm} \sim \frac{u_v + d_v}{4u_v + d_v}$$

constrain d/u

$$A_{\pm} = \frac{2}{P_R - P_L} \frac{\sigma_{\pm}(P_R) - \sigma_{\pm}(P_L)}{\sigma_{\pm}(P_R) + \sigma_{\pm}(P_L)}$$

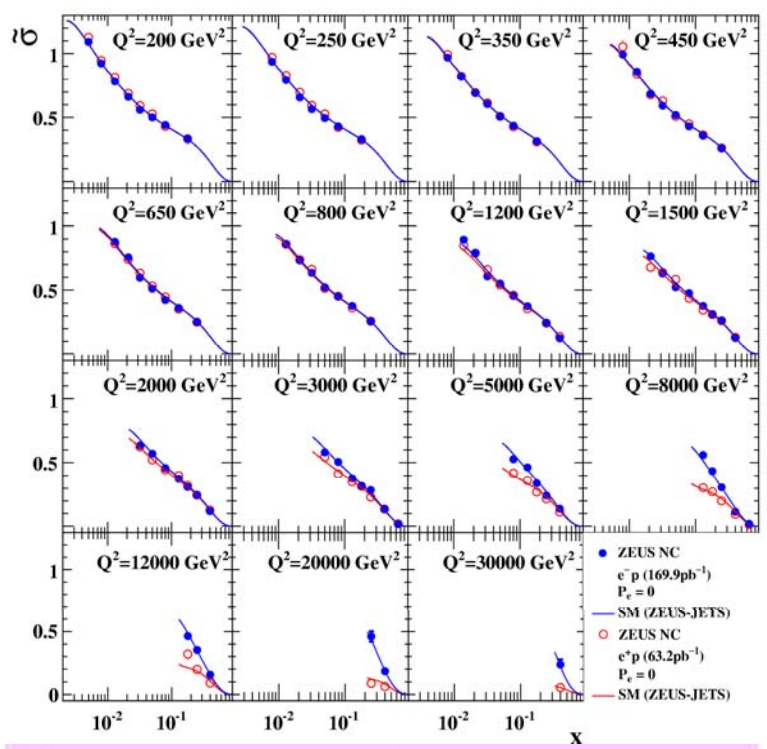


MPI Munich

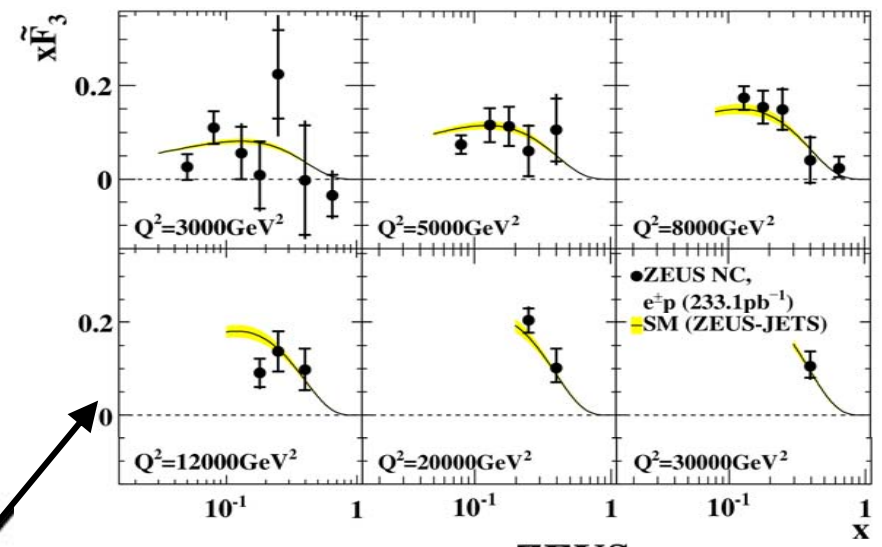
Burkard
 Reisert
 EINN 09
 Milos

A. Cooper-Sarkar

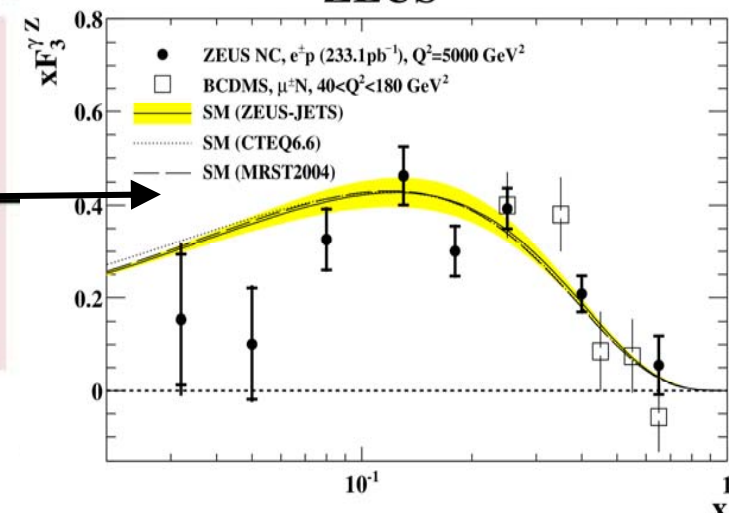
ZEUS



ZEUS



ZEUS



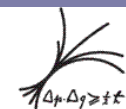
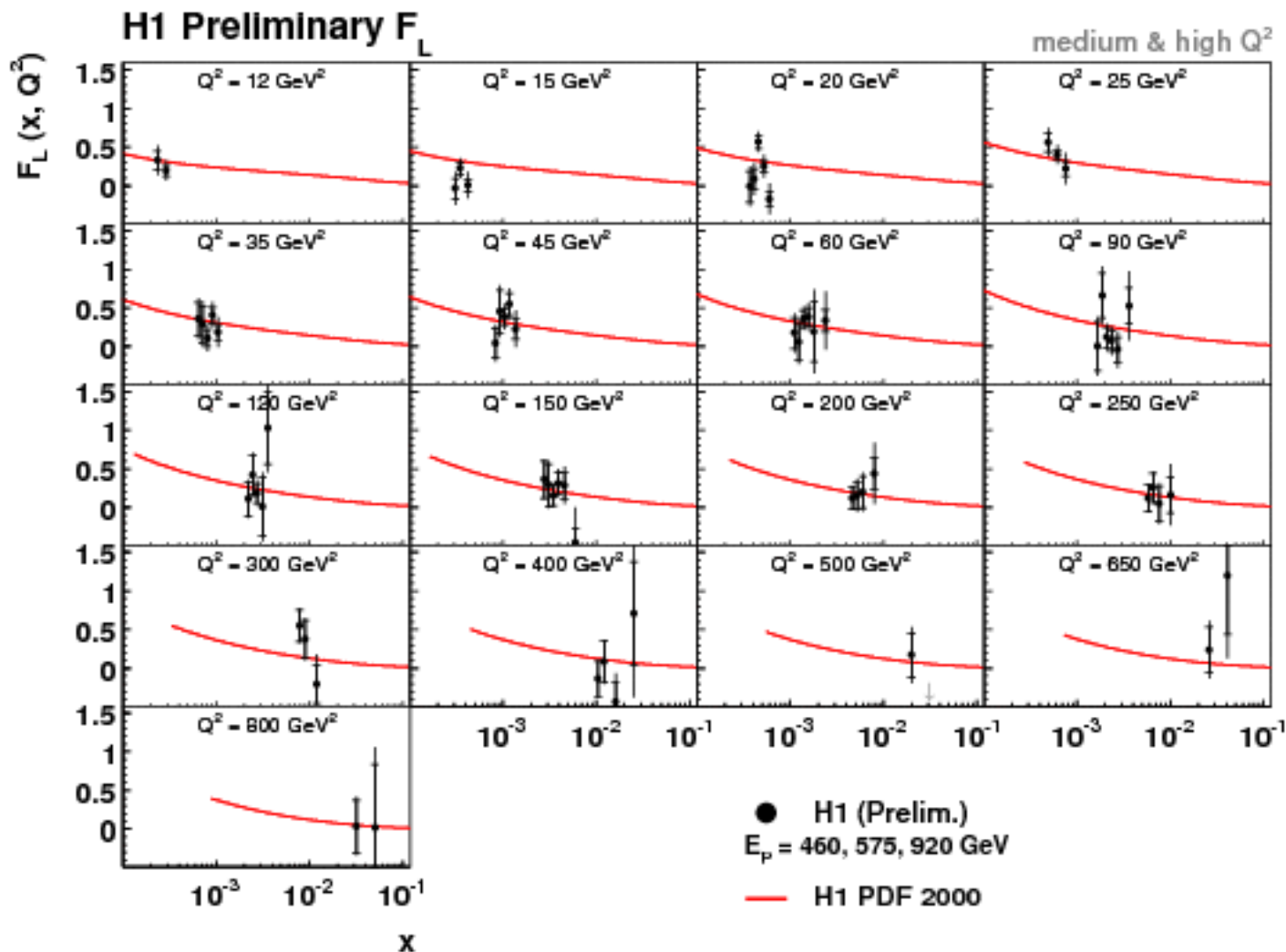
Compare these NEW e- NC data with HERA-I e+ NC data and use these two data sets to extract xF3

Much improved xF3 compared to previous extraction which used only 16.4 pb⁻¹ of e- NC data

Measurements from 1500 to 30000 GeV² have been extrapolated to 5000 GeV² to measure xF₃^{γZ} and compare to BCDMS at high-x

$$\frac{d^2\sigma(e\pm N)}{dx dy} = \frac{2\pi\alpha^2 s}{Q^4} \left[\frac{Y_+}{Y_+} [F_2(x, Q^2) - y^2 F_L(x, Q^2)] \pm \frac{Y_-}{Y_+} x F_3(x, Q^2) \right]$$

Extracted F_L – medium & high Q^2



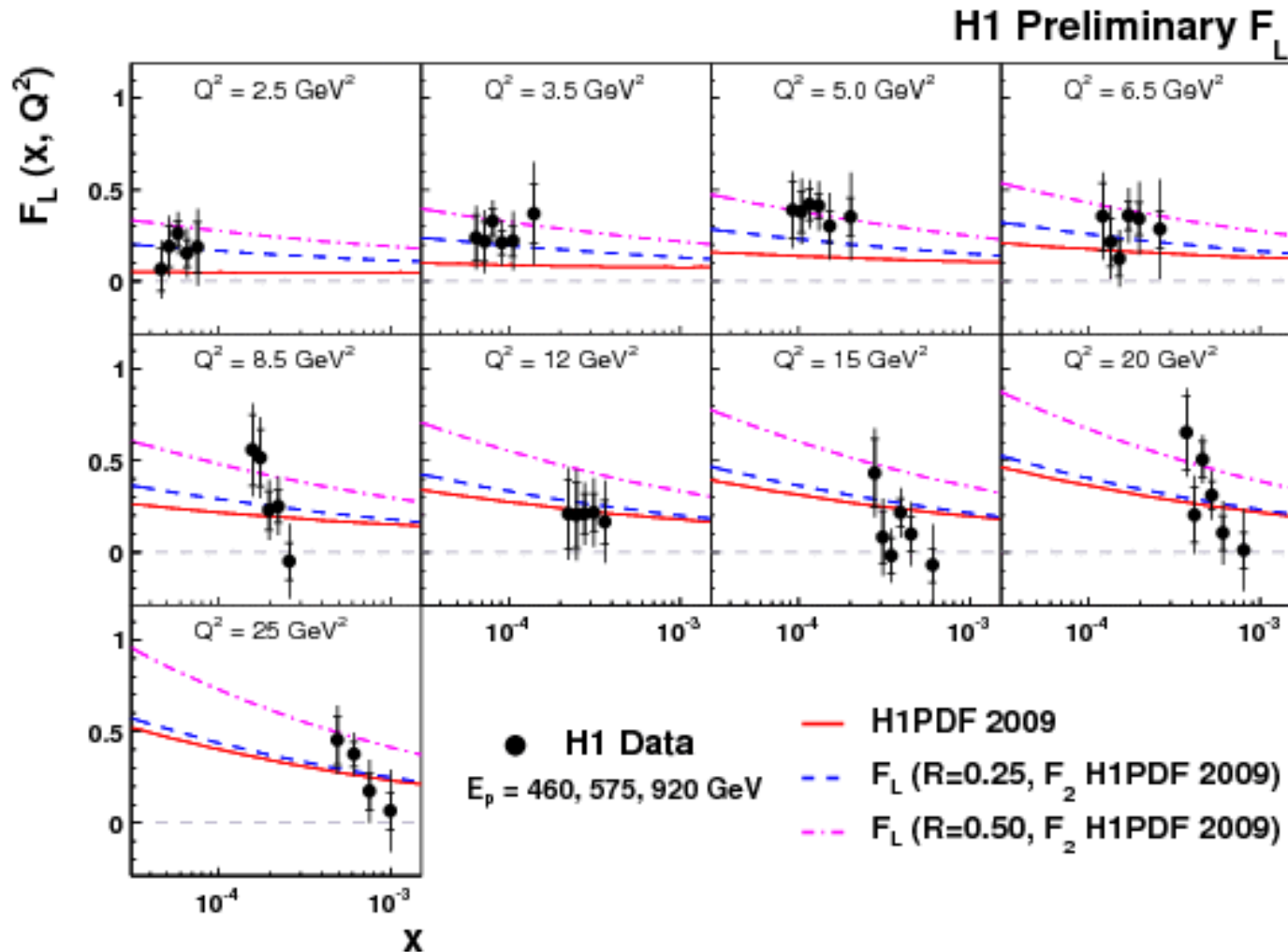
MPI Munich

Burkard
Reisert

DIS09
Low x & SF

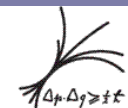
Medium Q^2 published in Phys. Lett. B665, p. 139

Extracted F_L – Low Q^2



F_L measured down to $Q^2 = 2.5 \text{ GeV}^2$!

Data are consistent with $R \sim 0.25$ ($F_L = 0.2 \cdot F_2$)

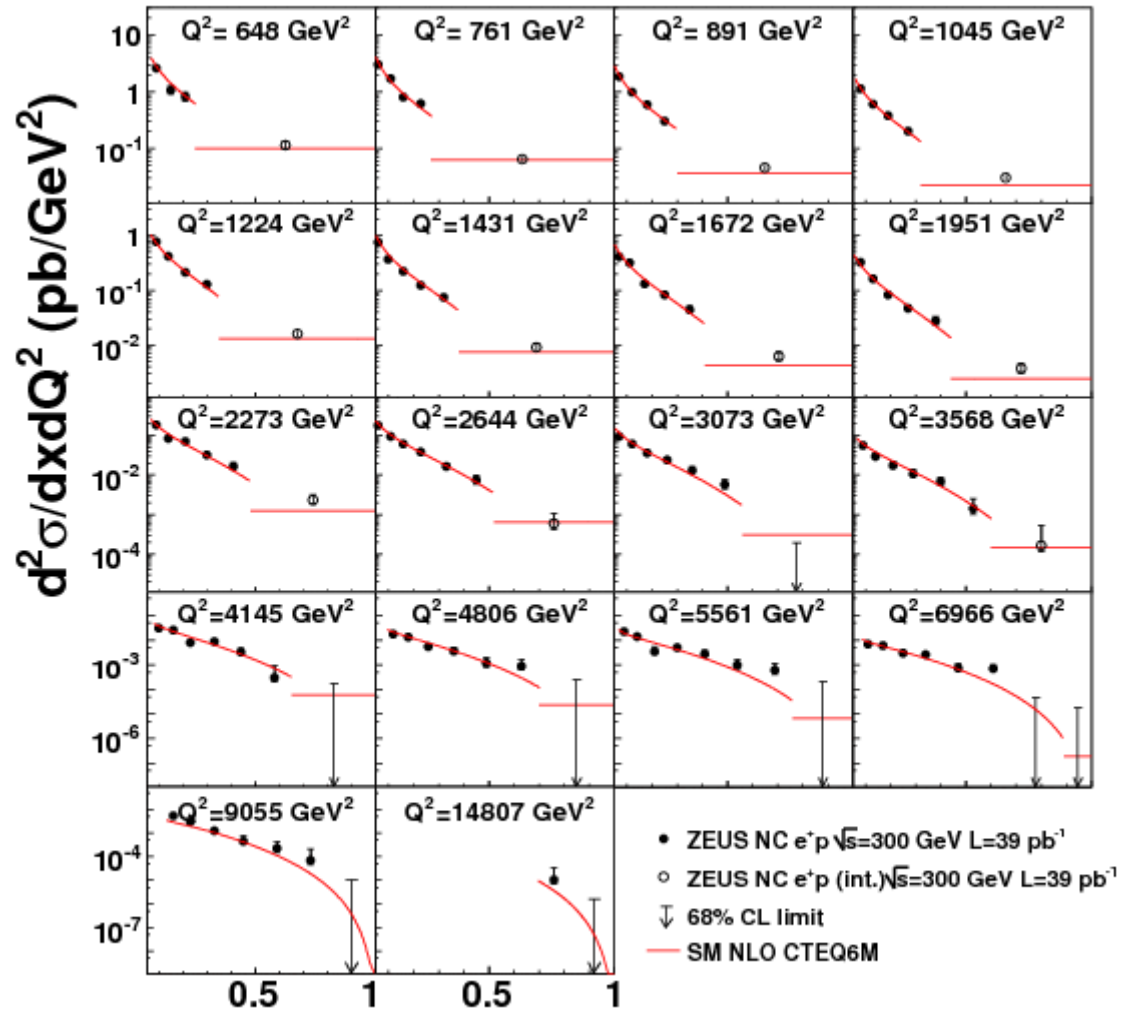


MPI Munich

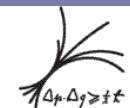
Burkard
Reisert

DIS09
Low x & SF

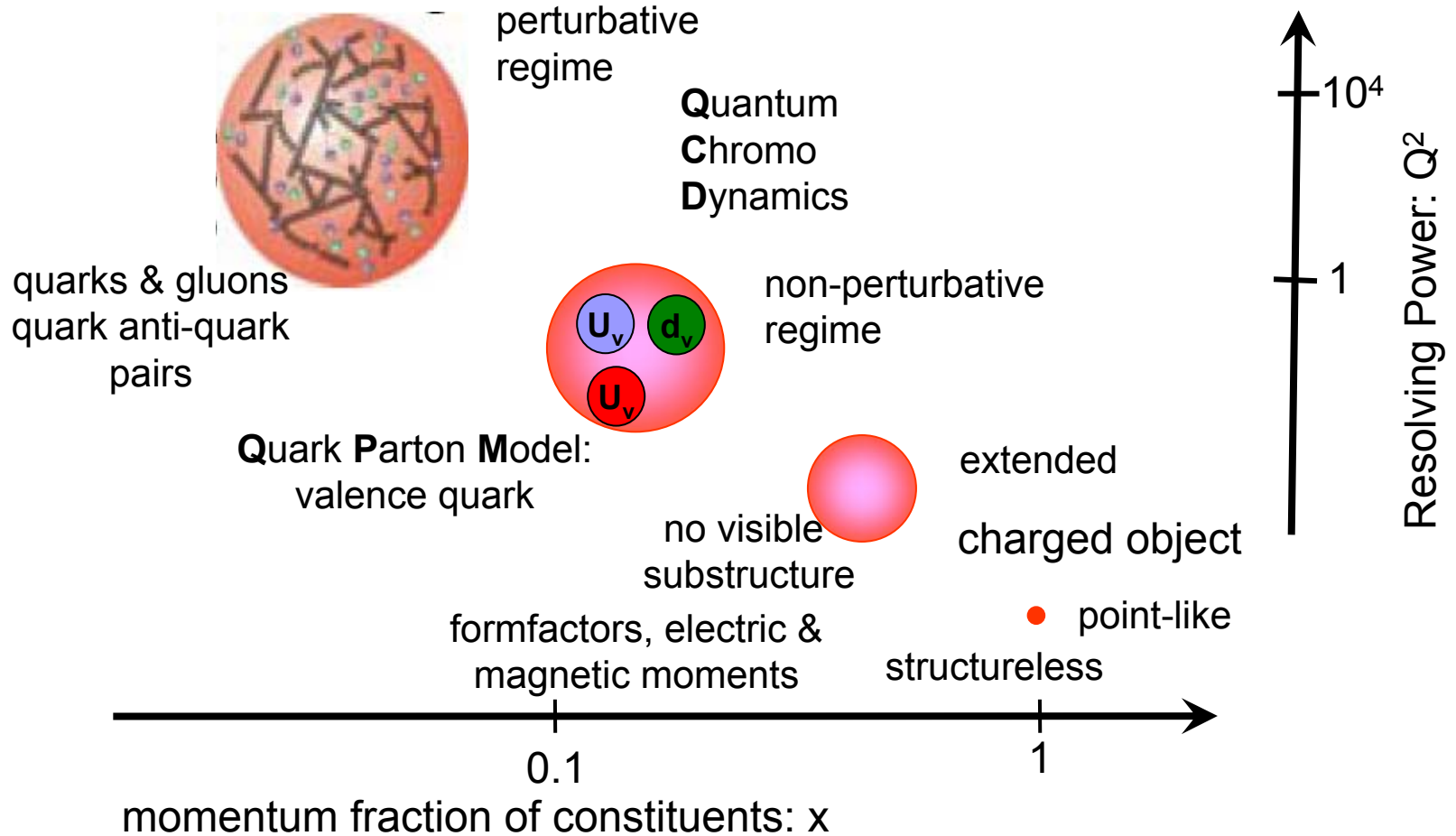
ZEUS



X



“Imaging” of the Proton



Low Q^2 : probing transition perturbative to non-perturbative QCD
 Low x : probing quarks and gluons at high density
 $\Delta E \Delta t \sim \hbar \rightarrow$ high Q^2 “high resolution but time averaged picture”

